OXFORD GENETICS

GENETICS, 2022, 222(1), iyac101
https://doi.org/10.1093/genetics/iyac101
Advance Access Publication Date: 6 July 2022
Investigation

Hox genes collaborate with helix–loop–helix factor Grainyhead to promote neuroblast apoptosis along the anterior–posterior axis of the *Drosophila* larval central nervous system

Rashmi Sipani [1,2], Rohit Joshi [1,*]

[1]Laboratory of Drosophila Neural Development, Centre for DNA Fingerprinting and Diagnostics (CDFD), Uppal, Hyderabad 500039, India,
[2]Graduate Studies, Manipal Academy of Higher Education, Manipal 576104, India

*Corresponding author: Laboratory of Drosophila Neural Development, Centre for DNA Fingerprinting and Diagnostics (CDFD), Inner Ring Road, Uppal, Hyderabad 500039, India. Email: rohit@cdfd.org.in; rj2152@gmail.com

Abstract

Hox genes code for a family of a homeodomain containing transcription factors that use TALE-HD containing factors Pbx/Exd and Meis/Homothorax to specify the development of the anterior–posterior axis of an organism. However, the absence of TALE-HD containing factors from specific tissues emphasizes the need to identify and validate new Hox cofactors. In *Drosophila* central nervous system, Hox executes segment-specific apoptosis of neural stem cells (neuroblasts) and neurons. In abdominal segments of larval central nervous system, Hox gene Abdominal-A mediates neuroblast apoptosis with the help of Extradenticle and bHLH factor Grainyhead using a 717-bp apoptotic enhancer. In this study, we show that this enhancer is critical for abdominal neuroblast apoptosis and relies on 2 separable set of DNA-binding motifs responsible for its initiation and maintenance. Our results also show that Abdominal-A and Grainyhead interact through their highly conserved DNA-binding domains, and the DNA-binding specificity of Abdominal-A-homeodomain is important for it to interact with Grainyhead and essential for it to execute neuroblast apoptosis in central nervous system. We also establish that Grainyhead is required for Hox-dependent neuroblast apoptosis in Labial and Sex Combs Reduced expressing regions of the central nervous system, and it can physically interact with all the Hox proteins in vitro. Our biochemical and functional data collectively support the idea that Grainyhead can function as a Hox cofactor and help them carry out their in vivo roles during development.

Keywords: HOX; Abdominal-A; Extradenticle; Grainyhead; neuroblast; apoptosis; *Drosophila*; enhancer; bHLH; homeodomain

Introduction

Hox genes code for a family of homeodomain (HD) containing transcription factors (TFs). They play an important role in the bilaterian anterior–posterior (AP) axis specification by executing different developmental programs along this axis (Hart *et al.* 1985; Regulski *et al.* 1985; Akam 1989; Carroll 1995). Conventionally, Hox factors are known to function with their TALE-HD containing cofactors Pbx and Meis in the vertebrates and Extradenticle (Exd) and Homothorax (Hth) in *Drosophila* (Mann and Chan 1996; Mann and Affolter 1998; Moens and Selleri 2006; Merabet *et al.* 2007; Lelli *et al.* 2011; Saadaoui *et al.* 2011; Hudry *et al.* 2012). These cofactors cooperatively bind with Hox on the target DNA and reveal its latent specificity, facilitating Hox's in vivo functions (Slattery *et al.* 2011; Merabet and Mann 2016). However, the broad expression of TALE factors and their absence or dispensability in specific tissues emphasizes the need to identify and validate new cofactors (Domsch *et al.* 2015; Saurin *et al.* 2018). In addition to Exd and Hth, the HD-containing factor Engrailed and the DM domain containing factor Doublesex (Dsx) are the only known cooperative cofactors for Hox genes (Gebelein *et al.* 2004; Ghosh *et al.* 2019). A handful of other TFs like Sloppy paired, Teashirt, Mad/Med help Hox factors to regulate their target genes, but these factors do not bind cooperatively with Hox on the DNA. They, therefore, are called collaborative cofactors (Mann *et al.* 2009). Recently, 3 studies have identified many more TFs with the potential to function as Hox cofactors in vivo (Baëza *et al.* 2015; Bischof *et al.* 2018; Carnesecchi *et al.* 2020).

In developing central nervous system (CNS), Hox genes generate a variety of different cell types and cell numbers along the AP axis by regulating proliferation, differentiation, and apoptosis of neural stem cells and their progeny (Prokop *et al.* 1998; Bello *et al.* 2003; Dasen *et al.* 2003; Economides *et al.* 2003; Miguel-Aliaga and Thor 2004; Dasen *et al.* 2005; Tabuse *et al.* 2011; Kuert *et al.* 2012; Birkholz *et al.* 2013; Kocak *et al.* 2013; Kuert *et al.* 2014). In *Drosophila*, CNS includes optic lobes, supraesophageal ganglia (SPG), subesophageal ganglia (SEG), and ventral nerve cord (VNC). The VNC has 3 thoracic (T1–T3), 7 abdominal (A1–A7), and 3 terminal (A8–A10) segments. The SPG, SEG, and VNC serially express different Hox genes and Hox-dependent neural stem cells [neuroblasts (NBs)] apoptosis in these regions play an important

Received: May 09, 2022. **Accepted:** June 21, 2022

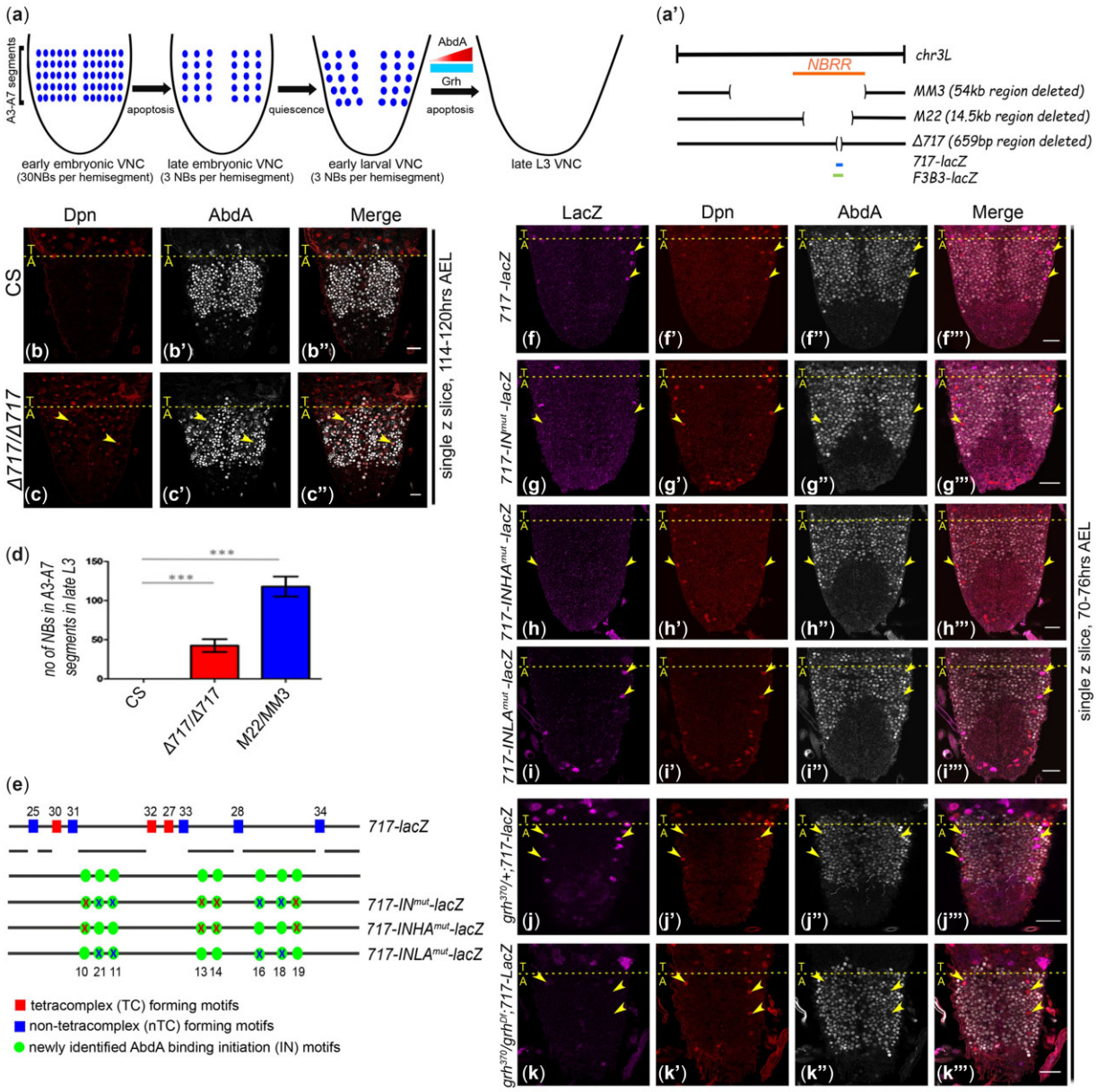

Fig. 1. The *717-enhancer* is necessary for abdominal NB apoptosis. a) Schematic representation of NB apoptosis in the abdominal region (A3–A7 segments) of embryonic and larval CNS. In early embryonic stages, each abdominal hemisegment has 30 NBs, this number is reduced to 3 NBs per hemisegment in the late embryonic stage, and reduced to zero NBs in the late L3 stage. The larval phase of abdominal NB apoptosis happens in response to increasing levels of AbdA and is facilitated by Grh. a') Shows the approximate location and extent of the *717-enhancer* (indicated by blue line) and *F3B3* (1Kb) enhancer (green line) relative to NBRR (light brown) and *MM3*, *M22*, and *Δ717* deletions. b) Abdominal region of control VNC from *Canton-S* (*CS*) show no NBs at late L3 stage. c) VNC homozygous for the deletion of the *717-enhancer* (*Δ717/Δ717*) show ectopic NBs (marked by Dpn) in abdominal segments at late L3 stage. d) The graph comparing the number of surviving abdominal NBs at the late L3 stage in controls (CS, 0 ± 0, $n = 17$ VNC and $N = 3$), *Δ717/Δ717* deletion (42.5 ± 8.2 NBs, $n = 17$ VNCs, $N = 3$), and *trans*-heterozygotes for *M22/MM3* deletions (117.9 ± 12.7 NBs; $n = 13$ VNCs, $N = 3$). e) A schematic representation of the *717-lacZ* showing the approximate position of motifs responsible for maintaining the enhancer activity in abdominal NBs (red and blue squares). The enhancer regions scanned for new AbdA-binding motifs (shown by green circles) are denoted by black lines. f–i) Comparison of lacZ expression at early L3 stage for wild-type (f–f‴; *717-lacZ*, $n = 10$, $N = 3$) and initiation motif mutagenized versions of the *717-enhancer*: *717-IN^{mut}-lacZ* (g–g‴; $n = 21$ VNCs, $N = 4$), *717-INHA^{mut}-lacZ* (h–h‴; $n = 12$ VNCs, $N = 3$); and *717-INLA^{mut}-lacZ* (i–i‴; $n = 16$ VNCs, $N = 3$). The data suggest that motifs showing strong AbdA binding are vital for initiation of the apoptotic enhancer. j–k) Comparison of the *717-lacZ* expression in early L3 stage in control (*grh^{370}/+*) vs. *grh* mutant (*grh^{370}/^{Df}*) VNCs, establishes the importance of Grh in the *717-enhancer* initiation. Yellow arrowheads indicate NBs. The yellow dotted line separates thoracic (T) and abdominal (A) segments of the VNC. AbdA staining show the approximate extent of the abdominal region in (b) and (c). Bar = 20μm. The graph shows mean ± SD. Significance is from a 2-tailed Student's unpaired *t*-test.

role in the patterning of the CNS in both embryonic and larval stages (Fig. 1a) (Prokop *et al.* 1998; Bello *et al.* 2003; Kuert *et al.* 2012; Birkholz *et al.* 2013; Kuert *et al.* 2014; Arya *et al.* 2015). In the larval CNS, Hox-dependent NB apoptosis has been reported in Labial (Lab) (Kuert *et al.* 2012), Deformed (Dfd) (Kuert *et al.* 2014), Sex combs reduced (Scr) (Kuert *et al.* 2014), Abdominal-A (AbdA) (Bello *et al.* 2003), and Abdominal-B (AbdB) (Birkholz *et al.* 2013; Ghosh *et al.* 2019; Bakshi *et al.* 2020) expressing regions.

The NBs in A3–A7 segments of larval CNS (hereon referred to as abdominal segments) undergo apoptosis in response to a dramatic increase in levels of AbdA at the mid-3rd instar larval stage (mid-L3) (Bello *et al.* 2003) (Fig. 1a). The helix–loop–helix (HLH) TF

Grainyhead (Grh) facilitates this process by conferring apoptotic competence to the NB and maintaining the expression of AbdA during the apoptosis (Cenci and Gould 2005). In addition to this, we had previously shown that AbdA, along with Notch signaling and Grh, critically requires Exd (but not Hth) to execute abdominal NB apoptosis (Khandelwal *et al.* 2017). These factors together activate transcription of the *RHG* family of apoptotic genes (*grim* and *reaper*) through an enhancer that lies within a 22 kb genomic region known as NBRR (NeuroBlast Regulatory Region, Fig. 1a′), which is located between genes *grim* and *reaper* (Tan *et al.* 2011; Arya *et al.* 2015). Using reporter LacZ assay and genomic deletions (which delete 54Kb-*MM3* and 14.5Kb-*M22* regions), we had narrowed down this enhancer to a 1-kb (*F3B3*) region and its 717-bp subfragment (*717-enhancer*) (Fig. 1a′) (Khandelwal *et al.* 2017). We identified 8 motifs on *717-enhancer* that could bind AbdA, Exd, and Grh. Our enhancer mutagenesis studies (wherein the Hox-, Exd-, and Grh-binding sites were mutated) indicated that these motifs are essential for maintaining enhancer activity in dying NBs, but do not have any role in initiating its activity in the early L3 stage (Khandelwal *et al.* 2017), an aspect that needs further investigation.

In contrast to the abdominal NBs, thoracic NBs (in T1–T3 and A1–A2 segments) do not undergo Hox-dependent apoptosis (Bello *et al.* 2003; Cenci and Gould 2005) since these NBs do not express resident Hox factor Antennapedia (Antp), or Ultrabithorax (Ubx). Instead, these cells undergo Prospero-dependent cell cycle exit (Bello *et al.* 2003; Cenci and Gould 2005; Maurange *et al.* 2008). However, since these cells express Grh (Cenci and Gould 2005) they are capable of undergoing apoptosis in response to ectopic expression of Hox factors (Antp, Ubx, AbdA, and AbdB; Bello *et al.* 2003; Ghosh *et al.* 2019). We have utilized this feature as a functional assay to identify different regions and residue(s) in Hox and Grh that are important for their interaction and role in NB apoptosis. Grh has been previously shown to play a critical role in Hox-dependent larval NB apoptosis in the abdominal (Cenci and Gould 2005), terminal (Bakshi *et al.* 2020), and Dfd expressing region of SEG (Khandelwal *et al.* 2017). However, its role in the Lab and Scr expressing regions of CNS (Lab-SPG and Scr-SEG) is yet to be tested.

In this body of work, we have dissected the molecular basis of abdominal NB apoptosis in the larval CNS. We find that a 717-bp enhancer is required for this apoptosis and relies on 2 sets of separable motifs to initiate and maintain its activity in NBs. Grh is a prerequisite for the AbdA-mediated initiation of the enhancer activity during apoptosis. Further, we show that AbdA-Exd interaction is essential for the apoptotic capacity of AbdA in the CNS. By conducting a systematic in vitro deletion analysis, we establish that AbdA and Grh interact through their highly conserved DNA-binding domains (DBD), and AbdA's DNA-binding specificity is vital for its apoptotic function. We also identify a pair of highly conserved arginine residues within Grh-DBD required for its DNA-binding and in vivo function. Lastly, we establish that Grh is an essential player for Hox-dependent NB apoptosis in the Lab-SPG and Scr-SEG regions, and it can physically interact with all the Hox proteins in vitro, supporting the idea that Grh can act as a Hox cofactor during development.

Material and methods

Fly stocks and fly husbandry

The following fly lines were used: Canton-S (BDSC-64349), grh^{RNAi} (VDRC-101428/KK), *exd-EGFP* (BDSC-81272), $labial^{01241}$-*lacZ* (BDSC-11527), *Df(2R)Pcl7B* (BDSC-3064), *UAS-Scr* (BDSC-7302), *UAS-Lab* (BDSC-7300), *UAS-dcr2; inscGAL4-UASmCD8-GFP; tub-GAL80^{ts}* (Neumüller *et al.* 2011), $grim^{A6C}$, *MM3*, *X25*, *XR38* (Tan *et al.* 2011), grh^{370} (Almeida and Bray 2005), *UAS-p35* (DGRC, Kyoto, 108019), *UAS-AbdA* on III, *UAS-Dfd*, *UAS-Scr*, *UAS-Ubx*, *UAS-AbdA-W1W2*, *UAS-AbdA* **Δ***UR*, *UAS-AbdA W1W2* **Δ***UR* (Lelli *et al.* 2011), *UAS-Antp* (this study), *UAS-AbdA* on II, *UAS-AbdA-Q50K* (Merabet *et al.* 2011), rpr^{17} (Ghosh *et al.* 2019), and *M22*, *F3B3-lacZ*, *717-LacZ* (Khandelwal *et al.* 2017). The generation of the **Δ***717* line was described earlier (Bakshi *et al.* 2020). $grim^{A6C}$-$labial^{01241}$-*lacZ*, *MM3-labial^{01241}-lacZ*, and $grim^{A6C}$-*GAL80^{ts}* recombinants were generated for this study. The transgenic lines for the mutagenized forms of the *717-lacZ* (TC^{mut}, nTC^{mut}, IN^{mut}, $INHA^{mut}$, and $INLA^{mut}$) were generated by site-specific insertion of the constructs at attP40-25C6. All the enhancer mutagenesis experiments were done in the *717-enhancer* to ensure that results in this study are comparable to our previous results (Khandelwal *et al.* 2017; Ghosh *et al.* 2019; Bakshi *et al.* 2020). The *717-lacZ* and *F3B3-lacZ* show similar expression pattern in larval CNS (Khandelwal *et al.* 2017), and were used interchangeably in experiments monitoring apoptosis induction. The choice of a specific line in the experiments (in Figs. 5 and 8) depended on the availability of relevant genetic strains. The genotypes analyzed in each figure are detailed in Section 8 of the Supplementary data.

The wild-type and mutagenized forms of GrhO (*UAS-GrhO′*, *UAS-GrhO*, *UAS-GrhO$^{R204/207A}$*, *UAS-GrhO-**Δ**DBD*, *UAS-GrhO-**Δ**183-208 DBD*), *UAS-AbdA-**Δ**HD*, and *UAS-Antp* were inserted at attP2-68A4. The following exd^{RNAi} (VDRC-7802/GD, 7803/GD, 100687/KK, and BDSC 29338, 34897) were tested by us. None of the exd^{RNAi} was potent enough to block abdominal NB apoptosis. Egg collections were done for 4 hr, and flies were grown at 25°C until desired time points of dissection. The L3 stage was divided into three 16-hr intervals to define the early, mid, and late L3 stage. The age was calculated as the number of hours after egg laying (AEL) and the larval age calculation for temperature-shift experiments is described below.

Temperature shift experiments

All temperature shift (TS) experiments used an inducible GAL4 system (IG4 system, *inscGAL4-UASmCD8-GFP*; *tub-GAL80^{ts}*) with stage-specific TS. The TS protocol for each experiment is mentioned in text and figure legends and schematized in Supplementary Fig. 3. The time of the TS is also indicated in the right margin of the figure panels. Six-hour egg collections were done for these experiments. The larvae were reared at 18°C till the desired stage and were then shifted to 30°C and dissected as per the requirement of each experiment.

Fly crosses were set up between virgin females of genotype, *UAS-dcr2*; *inscGAL4-UASmCD8-GFP*; *tub-GAL80^{ts}* and males of required genotype with appropriate controls (see Supplementary data 8 for detailed genotypes analyzed in each figure).

For the epistasis experiment, AbdA overexpression was done (from the late L2 to late L3 stage, TS, Supplementary Fig. 3b) in a genetic background that was homozygous for *grim* deletion and heterozygous for *rpr* deletion. The females of the genotype *inscGAL4-UASmCD8-GFP*; $grim^{A6C}$-*tub-GAL80^{ts}* were crossed to males of *UAS-abdA*; $grim^{A6C}$-rpr^{17} genotype. Longer AbdA induction was avoided as it resulted in sick larvae and poor survival.

For the experiments where apoptosis blocker p35 (LaCount *et al.* 2000) was used to block the NB apoptosis, the IG4 system was used to misexpress p35 from the late L1 to late L3 stage (TS, Supplementary Fig. 3a). This was to ensure that we recovered the maximum number of larval NBs.

For the experiment with simultaneous ectopic expression of AbdA and *grh* knockdown in thoracic NBs, the IG4 system was used from the late L1 stage to the late L3 stage (TS, Supplementary Fig. 3a). This was done to maximize the effect of *grh* knockdown during larval stages.

For the experiments where AbdA (or its mutant versions) or different Hox genes were ectopically expressed in thoracic NBs, the IG4 system was used to induce the expression for a short duration of 8 hr (from early L3 to mid-L3 stage, TS, Supplementary Fig. 3d), if lacZ expression had to be monitored (as longer AbdA expression causes NB apoptosis); and from late L2 till late L3 stage (TS, Supplementary Fig. 3b) if the apoptosis had to be monitored. Ectopic expression from the early L1 stage was avoided as it resulted in sick larvae and poor survival.

For the experiments where $AbdA^{Q50K}$ and Dfd were ectopically expressed in thoracic or abdominal NBs, the IG4 system was used to induce the expression from the late L1 to late L3 stage (TS, Supplementary Fig. 3a). This was to ensure that absence of apoptosis was not due to insufficient expression of $AbdA^{Q50K}$ and Dfd and to recover maximum number of surviving NBs in the abdominal region.

For the experiments where Grh and its mutant versions were overexpressed in thoracic or abdominal NBs, the IG4 system was used for overexpression from the early L1 to late L3 stage (TS, Supplementary Fig. 3c). This was to ensure that the absence of apoptosis was not due to insufficient expression of $Grh^{R204/207}$, and to recover any surviving NBs in the abdominal region.

Immunohistochemistry and image acquisition

CNS was dissected from larvae of the desired stage and fixed in 4% paraformaldehyde in 1× PBS containing 0.3% TritonX-100 for 30 min. The following primary antibodies were used: rabbit anti-Dpn (1/5,000; Bioklone, Chennai), rabbit anti-Grh (1/2,000; Bioklone), rabbit anti-Dfd (1/500, Bioklone), mouse anti-Grh (1/2,000), rat anti-Dpn (1/2,000), mouse anti-AbdA (1/2,000), mouse anti-Labial (1/2,000), chicken anti-β-gal (1/2,000, ab9361, Abcam), chicken anti-GFP (1/2,000, ab13970; Abcam), mouse anti-exd (1/20, B11M, DSHB, and this study), mouse anti-Scr (1/50, 6H4.1; DSHB), mouse anti-Antp (1/50, 8C11; DSHB), mouse anti-Ubx (1/50, FP3.38, DSHB), rabbit anti-Dcp1 (1/100, 9578; CST). N-terminal 6× His-tagged Labial protein (residues 207–514), and full-length Exd protein were used to raise antibodies in the mouse at the in-house animal facility. Secondary antibodies conjugated to Alexa fluorophores from Molecular Probes were used: AlexaFluor405 (1/250), AlexaFluor488 (1:500), AlexaFluor555 (1/1,000), and AlexaFluor647 (1/500). The samples were mounted in 70% glycerol. For TUNEL staining, mid-L3 CNS were dissected in 4% paraformaldehyde in 1× PBS for 30 min. Following primary antibody staining, the secondary antibody was diluted in the TUNEL reaction mixture (Roche in situ cell death detection kit; Fluorescein) and incubated overnight at 4°C and mounted in Vectashield (H-1000; Vector Labs) before imaging. Images were acquired with Zeiss LSM 700 confocal microscopes and processed using ImageJ and Adobe Photoshop CS2. Zen 2012 (blue edition) was used for intensity quantifications as previously described (Khandelwal *et al.* 2017). The NBs were counted manually in each slice in the region of interest while ensuring that no cell was counted twice. In all the experiments, a minimum of 10 VNCs were analyzed across a minimum of 3 technical replicates, and a representative confocal image is shown. Text on the right margin of the confocal panels indicate the age of the dissected larva (in "hr AEL") and whether image is a single confocal z-section or partial z project. The "*n*" represents the number of VNCs analyzed, and the "N" represents number of experimental repetitions in the text and figure legends. Bars = 20 μm unless stated otherwise in the figure legends. Yellow and pink arrowheads points NBs in all the figures except Supplementary Fig. 6b (where it points to low and high Exd expressing cells).

Microsoft Excel and GraphPad Prism were used for all the data analysis (an unpaired Student's *t*-test was done to check the significance of the data).

Electrophoretic Mobility Shift Assay (EMSA)

EMSAs were performed as previously described (Khandelwal *et al.* 2017). All DNA-binding experiments were performed with 6× His-tagged forms of Grh (residues 551–1,333), Grh R204/207A (residues 551–1,333), AbdA (residues 88–330), AbdA Q50K (residues 88–330), AbdA-W1W2ΔUR (residues 88–330), full-length Exd co-purified with HM domain of Hth, Dfd (residues 130–587), Antp (residues 1–362), Scr (residues 2-406), and GST–tagged Ubx (residues 1–381). Full-length Grh (1,333 residues) was truncated from the N-terminal till the start of exons 4 (exons 4 and 5 being specific to the CNS-specific isoforms). This truncated version is called GrhO-T and lacks 550 residues (shown in purple color in Fig. 3j) from the N-terminal region. His-tagged version of GrhO-T showed optimal bacterial expression and was used for both EMSA and GST-Pulldown assay.

GST-Pulldown assay

The following proteins were used for pulldown: GST, GST-AbdA (1–330 aa), GST-AbdA-Q50K(1–330 aa), GST-AbdA-W1W2ΔUR (1–330 aa), GST-Labial, GST-Dfd (3–585 aa), GST-Scr (1–407 aa), GST-Antp (1–379 aa), GST-Ubx (1–380 aa), GST-AbdB (89–270 aa), GST-AbdA-HD (138–197 aa), GST-AbdAΔN (1–138 aa were deleted), GST-AbdAΔΔN (1–197 aa were deleted), GST-AbdA-ΔHD (138–197 aa were deleted), GST-AbdAΔΔC (197–330 aa were deleted), 6×-His-exd (1–376 aa), 6×-His-GrhO-T (551–1,333 aa), 6×-His-exon4-DBD (551–1,132 aa), 6×-His-Δexon4 + 5 (756–1,333 aa), 6×-His-Grh-exon4 + 5 (551–756 aa), 6×-His-Grh DBD (873–11,32 aa), 6×-His-Grh ΔDBD (873–1,132 aa were deleted). For mapping residues within the AbdA-HD important for interaction with Grh, sequential 10 amino acid deletions were made within the HD (1–10, 11–20, 21–30, 31–40, 41–50, and 51–60 amino acids of the HD were deleted from GST-AbdA FL constructs). Similarly, for mapping residues within the Grh-DBD essential for interaction with AbdA, sequential 26 amino acids deletions within the Grh DBD were made (1–26, 27–52, 53–78, 79–104, 105–130, 131–156, 157–182, 183–208, 209–234, 235–260 amino acids of the DBD were deleted from the 6×-His-GrhO-T construct). GST-GrhO (1–1,333 aa) was used only for testing Grh and Exd interaction, owing to the poor expression often seen in the case of full length Grh. Bacterial cultures expressing full length/truncated GST-tagged and His-tagged proteins were induced for 4 h with 0.5 mM IPTG at 18°C. After sonication, lysates were subjected to Micrococcal Nuclease (MN) treatment at 30°C as described earlier (Nguyen and Goodrich 2006). Bead-bound GST proteins were incubated separately with an equal amount of His-tagged protein lysates for 2 hr at 4°C. Bead-bound proteins were separated by denaturing SDS-PAGE and then transferred onto PVDF membranes. The membrane was blocked in 5% milk in Tris-buffered saline with 0.1% Tween 20 (TBST). Primary antibody-mouse anti-His (H1029; Sigma-Aldrich) was diluted 1 in 5,000 in 5% milk in TBST, and the blot was incubated overnight at 4°C. The following HRP conjugated secondary antibody (Peroxidase-AffiniPure Rabbit Anti-Mouse IgG + IgM(H + L) (1/10,000, 315-035-048; Jackson Immunological Research Laboratory, USA) was used.

Visualization was carried out by enhanced chemiluminescence detection (34087-SuperSignal West Pico Chemiluminescent Substrate; ThermoFisher Scientific and K-12045-D20-Western Bright ECL kit; Advansta, USA). Representative blots from at least 3 repetitions of the experiments are shown in the figures. The figures indicate all the blots where the MN treatment was done for the lysate. All the Western Blots shown are from in-vitro pull-down experiments where bacterial lysates were used except those shown in Fig. 3g, where embryonic lysate was used in GST pulldown experiment and Fig. 3h, where *Drosophila* S2 cell lysates were used for pulldown with S-protein beads (detailed below).

GST-Pulldown using embryos

Canton-S stage 16 embryos were collected for 3-days, harvested, and lysed in lysis buffer containing 150 mM NaCl, 2 mM EDTA, 50 mM Tris, pH 7.5, and 0.1% NP-40. The resultant protein extract was subjected to preclearing by Glutathione Sepharose beads. 3 mg of the resultant precleared lysate was then incubated with GST-bound and GST-AbdAbo-und glutathione-sepharose beads overnight. 50 μg of protein was used as input. Bead-bound proteins were separated by denaturing SDS-PAGE, transferred onto nitrocellulose membrane, incubated with anti-Grh antibody (1:1,000) and detected with LI-COR Odyssey imaging system using goat antirabbit IRDye 680 LT (926-68021; LI-COR) secondary antibody. The same blot was then probed with an anti-GST antibody (B-14, sc138; Santa Cruz) and detected using goat antimouse IRDye 800 CW (926-32210; LI-COR) secondary antibody.

Pulldown in S2 cell culture

SFB-GFP and SFB-GrhO were cloned into the pRM-HA3 vector (gift from G. Ratnaparkhi). S2 cells (gift from R. Mishra) were seeded onto 6-cm plates and transfected with 5 μg of pRM-HA3-SFB-GFP and pRM-HA3-SFB-GrhO using Trans-IT insect reagent (MIR 6100, MIRUS) according to manufacturer's instructions. After 5 hr, the cells were induced with 500 μM $CuSO_4$ and harvested after 48 hr. The cells were lysed in NETN buffer (100 mM NaCl, 20 mM Tris, pH 7.5, 0.5 mM EDTA and 0.5% NP-40) and incubated with S-protein beads (69704; Novagen) for 2 h at 4°C. The beads were then washed thrice with pulldown wash buffer (15 mM Tris, pH 7.5, 100 mM KCl, and 0.01% NP40) and then loaded onto SDS-PAGE. After transfer, the blot was blocked with 5% milk and probed with anti-AbdA antibody (C-11, sc-390990; Santa Cruz) and anti-Flag antibody (F7425; Sigma).

Results

The *717-enhancer* is necessary for abdominal NB apoptosis

In the early larval stages, the abdominal (A3–A7) segments of the VNC collectively contain only 30 NBs (6 NBs per segment—3 per hemisegment) (Fig. 1a). The identifying feature of these cells is the expression of the NB marker Deadpan (Dpn) and their characteristic position in the abdominal segments of the larval VNC. AbdA-mediated apoptosis of these NBs begins in the mid-L3 stage of development (Supplementary Fig. 1, a and b), and all 30 NBs are eliminated by the late L3 stage (114–120 hr AEL; Fig. 1, a and b) (Truman and Bate 1988; Bello *et al.* 2003; Cenci and Gould 2005). We first investigated the hierarchical relationship between AbdA and apoptotic genes and found that *grim* and *rpr* are epistatic to AbdA in executing this cell death (Supplementary data 1 and Supplementary Fig. 1, c and d).

The *717-enhancer* is expressed in the abdominal NBs prior to their apoptosis (Khandelwal *et al.* 2017). To conclusively establish its role in cell death, we used a line deleted for the *717-enhancer* (Fig. 1a′) (Bakshi *et al.* 2020). We observed that abdominal NB apoptosis was abrogated in the homozygotes for the *717-enhancer* deletion (Δ*717*/Δ*717*) (Fig. 1b vs. Fig. 1c, and bar 2 in Fig. 1d). The block of apoptosis also led to a significant increase in the expression of the *717-lacZ* in the NBs, indicating that enhancer responds to feedback cues (Supplementary Fig. 1f vs. Supplementary Fig. 1g). We noted that surviving abdominal NBs in enhancer deletion homozygotes (Δ*717*/Δ*717*) were much lower than those in the genomic deficiency combination of *M22/MM3* (Fig. 1a′ and bar 3 in Fig. 1d). This suggested that the 14.5Kb region deleted in genomic deficiency *M22* (Khandelwal *et al.* 2017) contains multiple enhancers, some of which may be important for the death of embryonic NBs in the abdominal segments.

Collectively, these results establish a functional role for the *717-enhancer* in postembryonic abdominal NB apoptosis.

The *717-enhancer* initiation in abdominal NBs requires both Grh and AbdA

We had earlier identified 8 motifs responsible for maintaining the *717-enhancer* activity in dying NBs (Fig. 1e and Supplementary Fig. 2a). The mutagenesis of these motifs compromised the enhancer's capacity to maintain its expression in abdominal NBs in late larval stages as assessed by the *reporter-lacZ* assay (Supplementary Fig. 2f) (Khandelwal *et al.* 2017). However, the initiation of the enhancer in abdominal NBs was unaffected (Khandelwal *et al.* 2017). Three of these 8 maintenance motifs exhibit a tetracomplex assembly (DNA–AbdA–Exd–Grh) in electrophoretic mobility shift assay (EMSA) (Khandelwal *et al.* 2017) and are therefore referred to as TC motifs (red squares in Fig. 1e and Supplementary Fig. 2a). The remaining 5 motifs do not show tetracomplex assembly and are referred to as non-TC or nTC motifs (blue squares in Fig. 1e and Supplementary Fig. 2a) and only assemble a DNA–AbdA–Grh or DNA–AbdA–Exd complex (Khandelwal *et al.* 2017). The motifs responsible for the initiation of the enhancer had not been identified.

To test if the tetracomplex assembly observed in vitro correlated with the enhancer's maintenance activity in vivo, we checked the enhancer mutant for either TC or nTC motifs. We found that both TC and nTC motifs need to be mutagenized together to compromise the maintenance activity of the enhancer during NB apoptosis (Supplementary data 2, Supplementary Fig. 2, e–h and j); in other words, enhancer maintenance does not rely exclusively on TC motifs. This implies that tetracomplex (DNA–AbdA–Exd–Grh) is not the sole driver of the enhancer's maintenance activity, and DNA–AbdA–Exd and DNA–AbdA–Grh complexes are also likely to play an important role in this process.

Since the abdominal NB apoptosis happens in response to increasing levels of AbdA from early to mid-L3 stages, we expected the existence of additional AbdA-binding motifs responsible for the initiation of the apoptotic enhancer in the NBs. To this end, using EMSA, we systematically scanned the *717-enhancer* for the presence of new potential AbdA-binding sites (in the regions shown by bold lines in Fig. 1e), which were in addition to the previously identified maintenance motifs. We identified 8 new AbdA-binding motifs (green circles in Fig. 1e and Supplementary Fig. 4, a–j). These motifs were classified into "strong" and "weak" based on their intensity of binding with AbdA in EMSA assay. Mutation of these motifs dramatically reduced or abolished AbdA binding, indicating specificity (Supplementary Fig. 4, a–j). To test the role of these binding motifs in the initiation of the enhancer, we generated 3 *reporter-lacZ* lines. In the first line, all the new motifs were mutagenized (*717-IN^{mutant}-lacZ*). In the second and

third lines, we mutagenized the strong (*717-INHA^{mutant}-lacZ*) and weak (*717-INLA^{mutant}-lacZ*) binding motifs (Fig. 1e), respectively. We checked the expression of these lines in abdominal NBs at the early L3 stage. We observed that the *717-IN^{mutant}-lacZ* and the *717-INHA^{mutant}-lacZ* failed to initiate lacZ expression in abdominal NBs (Fig. 1f vs. Fig. 1, g and h), while the *717-INLA^{mutant}-lacZ* initiated expression normally in these cells (Fig. 1f vs. Fig. 1i). This established that strong AbdA-binding motifs were crucial for the *717-enhancer* initiation. We further established that the absence of lacZ expression at the early L3 stage in these cases (*717-IN^{mutant}-lacZ* and *717-INHA^{mutant}-lacZ*) was not due to the delay in initiation of the mutagenized enhancer (Supplementary data 3 and Supplementary Fig. 5, a–c).

Next, we tested the role of *grh* in enhancer initiation by checking the expression of the *717-lacZ* in a *grh* mutant background (*grh$^{370/Df}$*). This mutant combination survives till the late L3 stage despite severely reduced *grh* expression in CNS (Supplementary Fig. 5, e and f). We observed that in these mutants, the enhancer initiation in the early L3 stage was abrogated (Fig. 1j vs. Fig. 1k). We could not do a similar test for *exd*, as the *exd* mutants are embryonic lethal, and RNA interference (RNAi) lines are not strong enough to block abdominal NB apoptosis.

These results suggest that the *717-enhancer* has 2 separable sets of binding motifs responsible for its initiation and maintenance in abdominal NBs. We also find that Grh is required for AbdA-mediated *717-enhancer* initiation, and the tetracomplexes are vital but not the sole driver for the maintenance activity of the enhancer.

Interaction with Exd is essential for the apoptotic capacity of AbdA

Genetic studies have established that apoptosis of abdominal NBs requires the concerted activity of AbdA, Grh, and Exd (Bello *et al.* 2003; Cenci and Gould 2005; Khandelwal *et al.* 2017). While the expression of AbdA and Grh can be detected in the dying NBs (Khandelwal *et al.* 2017), we could not detect the expression of Exd (Supplementary data 4 and Supplementary Fig. 6a). Therefore, to check whether Exd has a direct role in the apoptosis of abdominal NBs, we tested an Exd protein trap line (BL81272, Exd-EGFP) and observed that we could use GFP as a good proxy for Exd expression in CNS (Supplementary data 4 and Supplementary Fig. 6b). Using this line, we could detect Exd expression in abdominal NBs just prior to initiation of apoptosis (in the early L3 stage, 70–74 hr AEL, Fig. 2a″). However, we failed to detect any expression before the early L3 stage (early and late L2 stage) or at the mid-L3 stage (Supplementary Fig. 6, c–e). This suggests that, like AbdA, perhaps Exd is also expressed in a pulse to induce the apoptosis of abdominal NBs.

AbdA is known to interact with Exd through highly conserved Tryptophan (W) containing Hexapeptide (HX) domains (TDWM-W1 and YPWM-W2; N-terminal to the HD) and UbdA and RRDR domains (UR; C-terminal to HD) (Merabet *et al.* 2007; Lelli *et al.* 2011; Saadaoui *et al.* 2011; Hudry *et al.* 2012) (Fig. 2b). To understand the role of these domains in facilitating the interaction of AbdA with Exd in developing CNS, we tested various versions of AbdA deleted for these domains for their capacity to bring about apoptosis of thoracic NBs. Inducible GAL4 system (detailed in material and methods) with stage-specific TS of the larvae (TS-temperature shift) was used to conditionally misexpress wild-type and different mutant versions of AbdA (from the late L2 to late L3 stage, TS, Supplementary Fig. 3b). We observed that compared to controls (Fig. 2c and bar 1 in Fig. 2h), both AbdA-W1W2 (Fig. 2e and bar 3 in Fig. 2h) and AbdA-ΔUR (Fig. 2f and bar 4 in Fig. 2h) caused thoracic NB apoptosis, like the wild-type AbdA (Fig. 2d and bar 2 in Fig. 2h). However, the apoptotic capacity of AbdA-W1W2ΔUR was compromised (Fig. 2g and bar 5 in Fig. 2h). This suggested that domains facilitating AbdA-Exd interaction are important for AbdA's capacity to induce apoptosis of thoracic NBs.

Next, we tested the importance of HX and UR domains in the biochemical assembly of the tetracomplex. For this, we compared the binding of the AbdA and AbdA-W1W2ΔUR with Exd and Grh in vitro on a previously characterized maintenance motif (motif-30) of the *717-enhancer*, which is known to assemble a robust tetracomplex of DNA–AbdA–Exd–Grh (Khandelwal *et al.* 2017) (Figs. 1e and 2j show the position and sequence of motif 30). We observed that while AbdA could form a complex with Exd (lanes 8–9, black arrowhead, Fig. 2i) and AbdA–Exd–Grh assembled a tetracomplex on motif 30 (lanes 12–13, pink arrowhead, Fig. 2i), AbdA-W1W2ΔUR failed to form either (lanes 21–22 and 25–26, Fig. 2j). However, HX and UR domains of AbdA were not critical for AbdA–Grh interaction in vitro (Supplementary data 5 and Supplementary Fig. 6f).

These results suggest that, like AbdA, Exd is transiently expressed in NBs prior to their apoptosis. The results also indicate that the conserved Exd interaction domains of AbdA are essential for tetracomplex assembly and are critical for AbdA to carry out its apoptotic role in developing CNS.

AbdA and Grh interact through their DNA-binding domains

Grh contributes to AbdA-mediated NB apoptosis in A3–A7 segments by stabilizing AbdA expression and conferring apoptotic competence to the NBs (Cenci and Gould 2005). To establish that Hox-induced thoracic NB apoptosis (in T1–T3 segments) relies on Grh, we ectopically expressed AbdA and simultaneously knocked down *grh* (from the late L1 to late L3 stage, TS, Supplementary Fig. 3a). We observed that *grh* knockdown compromised the ability of AbdA to bring about the apoptosis of thoracic NBs (Fig. 3d′ vs. Fig. 3c′ and bar 3 vs. 4 in Fig. 3e), as opposed to the expression of AbdA alone (Fig. 3c′ vs. Fig. 3a′ and bar 3 in Fig. 3e). Expectedly, the GFP expressing wild-type controls showed no NB apoptosis (Fig. 3a′, and bar 1 in Fig. 3e), and in the case of *grh* knockdown, we observed a slight increase in the number of thoracic NBs (bar 2, Fig. 3e), which is congruent with its role in supporting NB apoptosis. This observation suggests that AbdA and Grh collaborate in vivo to regulate apoptosis, an observation consistent with our previous results that AbdA and Grh physically interact with each other in vitro (Khandelwal *et al.* 2017).

Grh has 4 isoforms (O, O′ and N, N′), with "O" and "N" isoforms expressed in neural and nonneural tissues, respectively (Uv *et al.* 1997). The CNS-specific GrhO isoform has 2 additional coding exons (exons 4 and 5), and it differs from GrhO′ in having an additional exon 12b, which codes for a domain C-terminal to DBD of the protein (Fig. 3j). To validate AbdA–Grh interaction biochemically, we used a truncated version of GrhO (GrhO-T, lacking the first 550 residues, the purple region in Fig. 3j), which expressed better than full-length protein (1,333 residues).

We established the physical interaction between AbdA and Grh by the following three approaches. First, we performed an in vitro pulldown assay with bacterial lysates in the presence of Micrococcal Nuclease (MN) to rule out the role of bacterial DNA in mediating this interaction (Fig. 3f). We observed that AbdA–Grh interaction was stable in the presence of MN treatment (lane 3, Fig. 3f). We then validated this interaction in the embryos, wherein we observed that GST-AbdA could pull down endogenous Grh from embryonic lysate while GST alone could not (lane

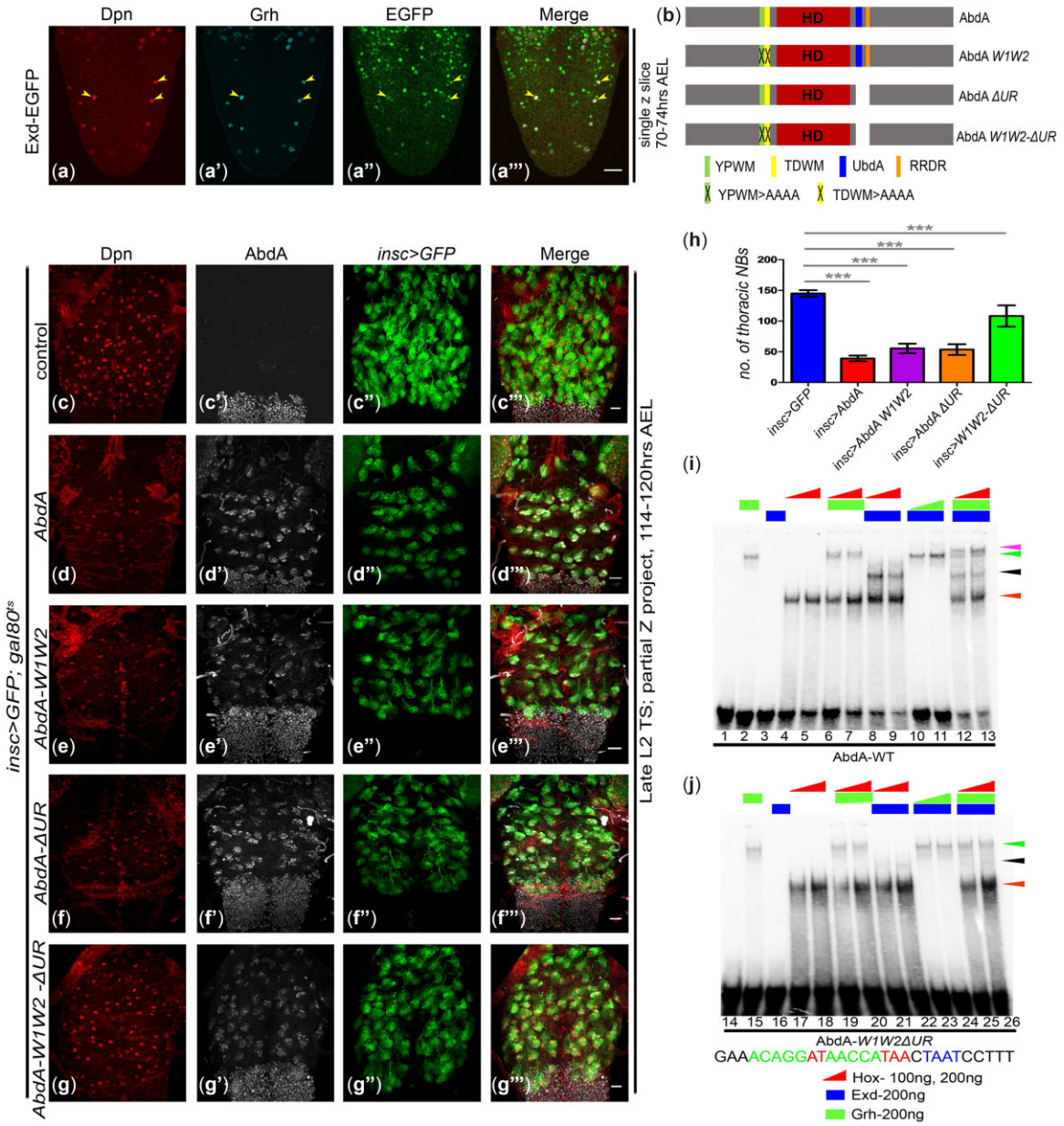

Fig. 2. Exd interaction is essential for the apoptotic function of AbdA. a) The expression of Exd-EGFP fusion protein in abdominal NBs at early L3 stages prior to apoptosis. b) Schematic showing the position of various Exd-interaction domains relative to the HD (shown in red) in wild-type AbdA. W1 and W2 correspond to the YPWM (green) and TDWM (yellow) domains, U and R represents the UbdA (blue) and RRDR (orange) domain, respectively. Three mutagenized versions of AbdA used are also shown. The first version had both the TDWM and YPWM domains mutated to alanine residues (AAAA) (AbdA-W1W2); the second had the UbdA and RRDR domains deleted (AbdA-ΔUR), and the third had both YPWM and TDWM mutated and UbdA and RRDR domains deleted (AbdA-W1W2ΔUR). c–g) Comparison of the surviving thoracic NBs show that mutation/deletion of all Exd interaction domains of AbdA (AbdAW1W2-ΔUR) compromises its apoptotic potential. The ectopic expression of AbdA and its mutants versions was done from late L2 to late L3 stage (TS, Supplementary Fig. 3b). h) The graph compares the number of surviving thoracic NBs upon the ectopic expression of the various mutant versions of AbdA shown in (c)–(g) (*insc>GFP*: 145.5 ± 7.1 NBs, $n = 21$ VNCs, $N = 5$ vs; *insc>AbdA*: 39.2 ± 4.7 NBs, $n = 22$ VNCs, $N = 5$; *insc>AbdA-W1W2*: 53.7 ± 8.7 NBs, $n = 25$ VNCs, $N = 5$; *insc>AbdAΔUR*: 55.5 ± 7.7 NBs, $n = 22$ VNCs, $N = 3$; *insc>AbdAW1W2-ΔUR*: 108 ± 16.8 NBs, $n = 21$ VNCs, $N = 5$). i–j) EMSAs for the binding of wild-type AbdA and AbdA-W1W2-ΔUR with Exd and Grh on motif 30 of the *717-enhancer*. i) AbdA forms Hox-Exd-DNA complex (lanes 8–9, black arrowhead) and Hox–Exd–Grh–DNA tetracomplex (lanes 12–13, pink arrowhead). j) AbdA-W1W2-ΔUR, can bind DNA on its own (red arrowhead) but is incapable of forming Hox-Exd-DNA (lanes 21–22, black arrowhead) or Hox–Exd–Grh–DNA tetracomplex (lanes 25–26). Rectangles show a fixed concentration of 200 ng of Exd (blue), and Grh (green); the right triangle shows increasing concentrations of 100 and 200 ng for Hox (red). The DNA sequence used for both EMSA experiments is given at the bottom of (j). Protein added in EMSA is shown on the top of each lane. Red, black, green, and pink arrowheads show Hox–DNA, Hox–Exd–DNA, Hox–Grh–DNA, and Hox–Exd–Grh–DNA complexes. Yellow arrowheads indicate NBs. Bar = 20μm. TS stands for "temperature shift." The graph shows mean ± SD. Significance is from a 2-tailed Student's unpaired *t*-test.

6 vs. 7, Fig. 3g). Lastly, we tested AbdA–Grh interaction ex vivo in S2 cells. We used full-length GrhO tagged with SFB (S-protein FLAG-streptavidin-binding peptide). We observed that while SFB-Grh could pull down endogenous AbdA, SFB-GFP could not do so (lane 9 vs. 10 in Fig. 3h). These results collectively show that AbdA physically interacts with Grh in vivo.

Next, we used the in vitro pulldown assay done with bacterial lysates of large deletions in AbdA and Grh (detailed in Fig. 3, i and j)

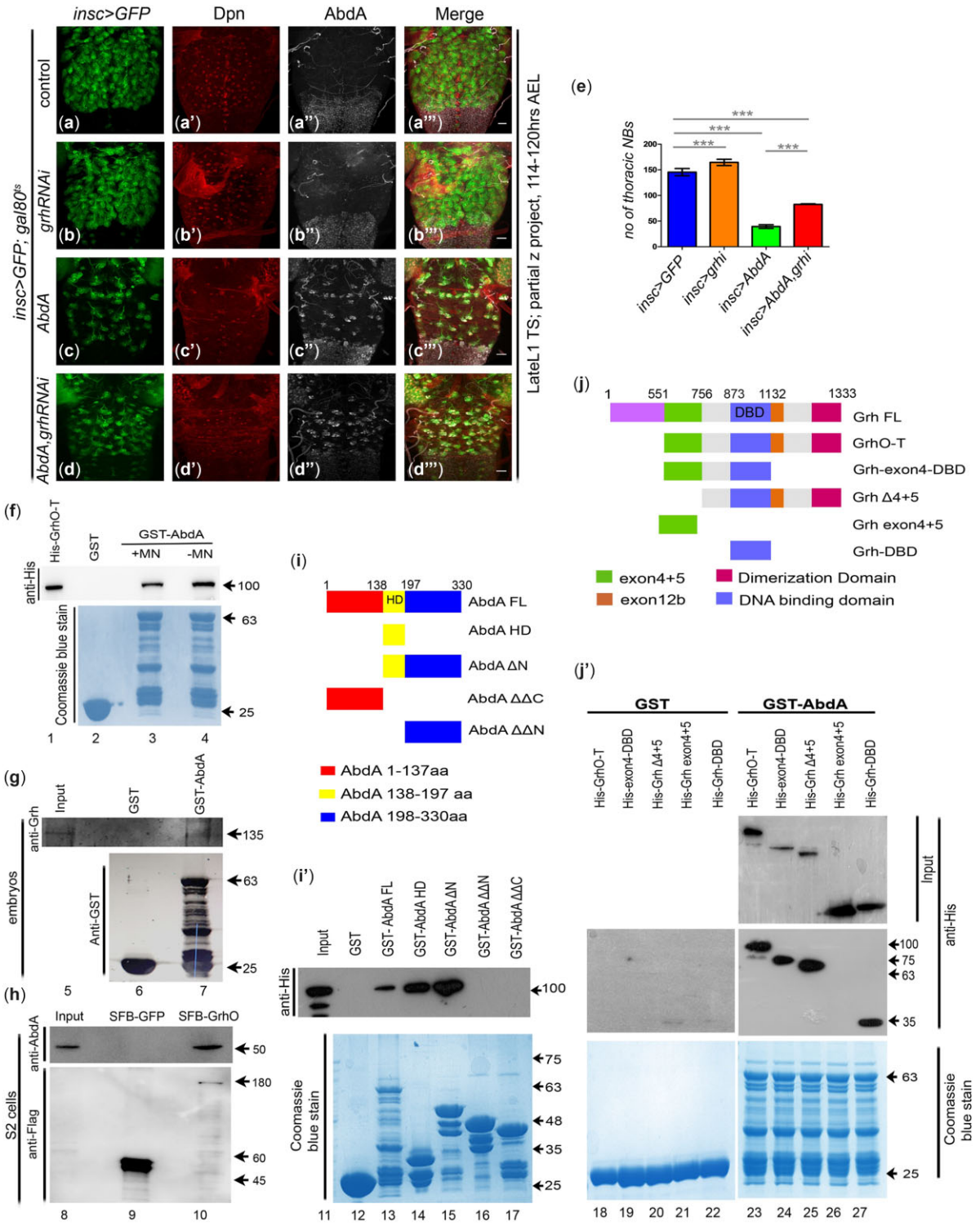

Fig. 3. AbdA and Grh interact through their DNA-binding domains. a–d) Comparison of the surviving NBs in thoracic region of the VNC shows that simultaneous knockdown of *grh* with ectopic expression of AbdA compromises the potency of AbdA-mediated NB apoptosis. The knockdown and ectopic expression were induced from the late L1 to late L3 stage (TS, Supplementary Fig. 3a). e) The graph compares the number of thoracic NBs surviving in the VNCs for different genotypes analyzed in (a)–(d) (*insc>GFP*: 145.1 ± 6.5 NBs, $n = 12$ VNCs, $N = 3$ vs. *insc> grhRNAi*: 164.5 ± 4.06 NBs, $n = 10$ VNCs, $N = 3$; *insc>AbdA*: 39.45 ± 3.9 NBs, $n = 12$ VNCs, $N = 3$; *insc>AbdA, grhRNAi*: 82.6 ± 3.9 NBs, $n = 13$ VNCs, $N = 3$). f) Western blot shows that the interaction between AbdA and Grh is stable even in the presence of Micrococcal Nuclease (denoted as +MN) treatment (lane 3 vs. 4), indicating that bacterial DNA does not mediate this interaction. g) Western blot shows that GST-AbdA, but not GST alone could pull down Grh from stage 16 embryonic lysate (lane 6 vs. 7). h) Western blot shows that SFB tagged Grh could pull down endogenous AbdA from S2 cell lysates, while SFB-GFP could not do the same (lane 9 vs. 10). i–j) The schematic of various GST-tagged AbdA and His-tagged Grh versions used for mapping AbdA–Grh interaction domain/s in vitro. i') Western blot for the interaction of bacterially expressed GrhO-T with full length and domain deleted versions of AbdA, show that AbdA-HD is required for interaction with Grh (lane 14). j') Western blot for bacterially expressed full-length AbdA with various domain deleted versions of Grh, show that DBD of Grh is required for interaction with AbdA (lane 27). Coomassie Blue gel depicts the loading of the GST-tagged protein samples. Bar = 20 μm. The graph shows mean ± SD. Significance is from a 2-tailed Student's unpaired *t*-test.

to identify the specific domain/s responsible for their interaction. Our results indicated that HD of AbdA and DBD of Grh are the primary determinants of this interaction (Fig. 3, i′ and j′, Supplementary data 6). To check the criticality of these 2 domains, we made internal deletions of AbdA-HD (AbdA-ΔHD, Fig. 4a) and Grh-DBD (Grh-ΔDBD, Fig. 4e), and tested their interaction with Grh and AbdA, respectively. Our result suggests that while the Grh-DBD plays a vital role in its interaction with AbdA (lane 15, Fig. 4e′); AbdA-HD though necessary (lane 3, Fig. 4a′), is not the sole determinant for AbdA–Grh interaction, and additional residues outside the AbdA-HD may also be required for this interaction.

Subsequently, we wanted to map the amino acids (within AbdA-HD and Grh-DBD) responsible for AbdA–Grh interaction. For this, we made consecutive nonoverlapping deletions spanning the AbdA-HD (6 deletions of 10 amino acids each) (Fig. 4a′) and Grh-DBD (10 deletions of 26 amino acids, Supplementary Fig. 7a) and tested them for their interaction with Grh and AbdA, respectively. None of the internal deletions within AbdA-HD were sufficient to abolish the AbdA–Grh interaction (lanes 4–9, Fig. 4a′). However, the deletion of 2 stretches of residues (27–52 and 183–208) within Grh-DBD resulted in the loss of AbdA–Grh interaction (lane 20 vs. 21, Fig. 4e″ and lane 3 vs. 4, Supplementary Fig. 7a).

We functionally validated these results in vivo by misexpressing the following in the thoracic NBs: HD-deleted AbdA (AbdA-ΔHD), DBD-deleted Grh (Grh-ΔDBD), and Grh with residues 183–208 deleted in DBD (Grh-Δ183–208). The residues 183–208 were chosen over residues 27–52 of Grh-DBD, owing to their high conservation (discussed later). We observed that ectopic expression of AbdA (from the late L2 to late L3 stage, TS, Supplementary Fig. 3b) results in thoracic NB apoptosis (Fig. 4d′ and bar 3 in Fig. 4j), however, the overexpression of AbdA-ΔHD was incapable of causing the same (Fig. 4c′ and bar 2 in Fig. 4j). Similarly, while the overexpression of GrhO (from late L1 to L3 stage, TS, Supplementary Fig. 3a) led to a mild reduction in the number of thoracic NBs, GrhO-Δ183–208 (Fig. 4h′ and bar 3 in Fig. 4k) and GrhO-ΔDBD (Fig. 4i′ and bar 4 in Fig. 4k) caused a slight but significant increase in the number of thoracic NBs, suggesting that AbdA-HD and Grh-DBD are crucial for the execution of AbdA and Grh functions in vivo. The results with Grh corroborate our previous observation wherein *grh* knockdown (shown in Fig. 3, b and e) causes a slight but consistent increase in the number of thoracic NBs, suggesting the existence of Grh-dependent apoptosis of some NBs in the thoracic region. The apoptosis induced by Grh overexpression could be because Grh can function as a pioneer TF (Nevil *et al.* 2017; Jacobs *et al.* 2018; Nevil *et al.* 2020). Therefore, its levels need to be tightly regulated, and its overexpression could cause nonspecific target gene activation leading to cell death.

These results collectively indicate that AbdA and Grh interact through their highly conserved HD and DBD. Furthermore, the deletion of these domains was sufficient to dramatically reduce the AbdA–Grh interaction and compromise the in vivo functions of these proteins.

Q50K mutation in AbdA-HD changes its DNA-binding specificity and compromises its apoptotic potential

Gln50 (Q50) in the third helix of the HD contacts DNA in the major groove and is essential for the DNA-binding specificity of the Antp class of HDs (Treisman *et al.* 1989; Affolter *et al.* 1990; Noyes *et al.* 2008). To test if the DNA-binding specificity of AbdA-HD was crucial for its apoptotic potential, we tested a mutagenized version of AbdA, where Q50 was replaced with a lysine residue ($AbdA^{Q50K}$). This mutation switches the DNA-binding specificity of the Antp class of HD to that of the bicoid class of HD (Treisman *et al.* 1989; Affolter *et al.* 1990; Noyes *et al.* 2008) without abrogating its DNA-binding capacity.

We observed that while wild-type AbdA bound to motif 30 of the *717-enhancer* (lanes 2–4, Fig. 5a), it did not show binding on the bicoid consensus site (TCTAATCCC) (Lebrecht *et al.* 2005) (lanes 9–11, Fig. 5a′). In contrast, the Q50K mutation abolished AbdA's capacity to bind on motif 30 (lanes 5–7, Fig. 5a), but the mutant protein bound efficiently on the bicoid consensus site (lanes 12–14, Fig. 5a′).

Since $AbdA^{Q50K}$ could not bind to motif 30, we checked if its overexpression could induce the expression of *F3B3-lacZ* and if longer induction results in apoptosis of the thoracic NBs. Expectedly, we observed that the ectopic expression of AbdA (for 8 hr from early L3 to the mid-L3 stage, TS, Supplementary Fig. 3d) led to a dramatic increase in expression of *F3B3-lacZ* in the central brain and thoracic region of the VNC (Fig. 5b′ vs. Fig. 5c′) (Khandelwal *et al.* 2017). However, overexpression of $AbdA^{Q50K}$ did not result in induction of *F3B3-lacZ* (Fig. 5b′ vs. Fig. 5c′ vs. Fig. 5d′).

Similarly, in contrast to wild-type AbdA (Fig. 2d, bar 3 in Fig. 5i), ectopic expression of $AbdA^{Q50K}$ (from the late L1 to late L3 stage, TS, Supplementary Fig. 3a) was incapable of causing thoracic NB apoptosis (Fig. 5e vs. Fig. 5f and bar 2 in Fig. 5i). Interestingly, we also observed that overexpression of $AbdA^{Q50K}$ in abdominal NBs could partially block their apoptosis (Fig. 5h′), with approximately 10 out of 30 NBs surviving in a late L3 VNC ($n = 12$ VNCs, $N = 3$), compared to control VNCs, where all NBs have been eliminated by the late L3 stage (Fig. 5g′). This led us to check if the Q50K mutation in AbdA affected its interaction with Exd and Grh. We observed that as compared to wild-type AbdA, the interaction of $AbdA^{Q50K}$ was significantly reduced with Exd (compare lane 3 vs. 4, Fig. 5j) and lost in the case of Grh (compare lane 7 vs. 8, Fig. 5j′). Furthermore, both $AbdA^{Q50K}$ and AbdA-ΔHD showed a similar reduction in their interaction with Grh (lane 15 vs. 16 and 17, Supplementary Fig. 7b). We also observed that Exd and Grh interact with each other (Supplementary Fig. 6g), suggesting that the interaction of Grh with both AbdA and Exd contributes to the assembly of the transcriptional complex.

These results collectively indicate that the DNA-binding specificity of AbdA is essential for its in vivo apoptotic potential. The change in the DNA-binding specificity significantly affects AbdA's interaction with Exd and Grh, which may affect the transcriptional activation of apoptotic genes during abdominal NB apoptosis.

R204/207 of Grh-DBD are essential for its DNA binding and in vivo function

A recent study elucidating a crystal structure of the vertebrate homologs of *Drosophila* Grh (Grhl1 and 2) had identified 2 arginine residues (R427 and R430) important for target DNA recognition (Ming *et al.* 2018). The R427 and R430 correspond to R204 and R207 in the *Drosophila* Grh-DBD and lie within the stretch of residues (183–208), which show high cross phylum conservation (Fig. 6a). This stretch of residues is crucial for in vivo function of GrhO and its capacity to interact with AbdA (Fig. 4, f″–i″). We mutagenized these arginine residues ($GrhO^{R204/207A}$) and observed that unlike wild-type GrhO (lanes 2 and 3, Fig. 6g), the mutant protein fails to bind to motif 30 of the *717-enhancer* (lanes 4 and 5, Fig. 6g).

In order to test the in vivo role of R204/207 residues, we overexpressed GrhO and $GrhO^{R204/207A}$ in thoracic NBs (from early L1 to the late L3 stage, TS, Supplementary Fig. 3c). Independently,

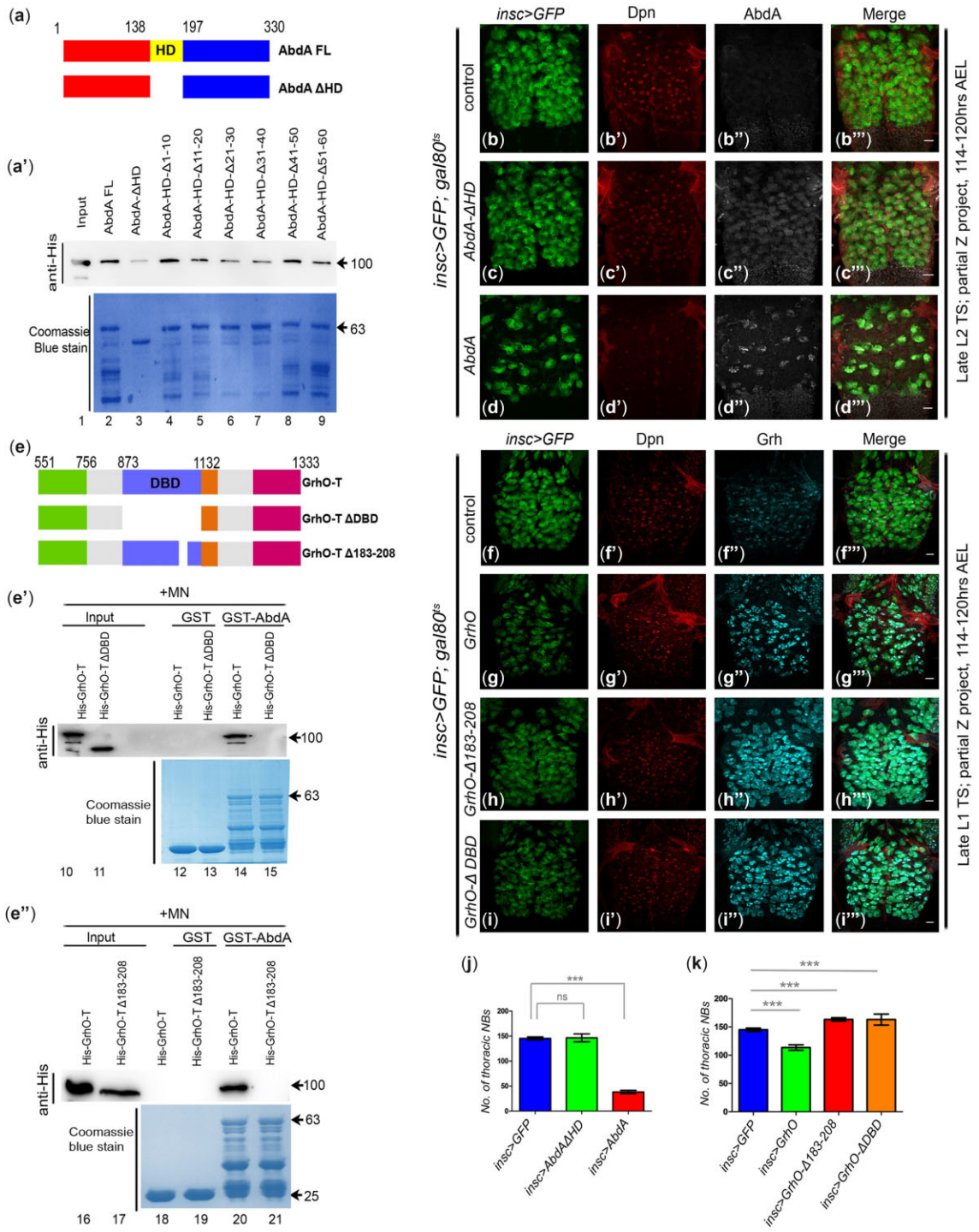

Fig. 4. Residues 183–208 of the Grh-DBD are crucial for its interaction with AbdA. a and e) The schematic of the HD-deleted AbdA and DBD-deleted Grh used for the GST-Pulldown assays. a′) Western blot showing various internal deletions within AbdA-HD tested for their interaction with Grh. The deletion of the entire AbdA-HD significantly reduce but do not completely abrogate its interaction with Grh (lane 3), suggesting that additional regions outside HD may also mediate this interaction. None of the internal deletions within the HD could parallel the reduction observed in case of the entire HD deletion (lanes 4–9). b–d) Comparison of surviving thoracic NBs show that deletion of AbdA-HD compromises its apoptotic potential (*insc>GFP*: 145.3 ± 3.1 NBs, $n = 13$, $N = 3$ vs. *insc>AbdA*: 38.1 ± 3.3 NBs, $n = 13$, $N = 4$; *insc>AbdAΔHD*: 146.5 ± 7.5 NBs, $n = 12$, $N = 3$). e′) Western blot showing that deletion of DBD of Grh disrupts Grh–AbdA interaction in vitro (lanes 14–15). e″) Western blot showing that residues 183–208 of Grh-DBD (lane 20 vs. 21) are essential for its interaction with AbdA in vitro. f–i) Comparison of surviving thoracic NBs show that deletion of GrhO-DBD or residues 183–208 of Grh-DBD compromises its apoptotic potential (*insc>GFP*: 145 ± 2.9 NBs, $n = 12$, $N = 3$ vs. *insc>GrhO*: 113.6 ± 4.8 NBs, $n = 11$, $N = 3$; *insc>GrhO-Δ183–208*: 163.2 ± 3 NBs, $n = 11$, $N = 3$; *insc>GrhO-ΔDBD*: 163 ± 9.67 NBs, $n = 10$, $N = 3$). The graphs comparing the number of surviving thoracic NBs upon the ectopic expression of GFP (controls), wild-type AbdA and AbdA-ΔHD (j) and wild-type GrhO, GrhO-ΔDBD, and GrhO-Δ183–208 (k). AbdA and its mutant versions were ectopically expressed for a shorter interval (from late L2 to late L3 stage, TS, Supplementary Fig. 3b) owing to poor survival of larvae. GrhO and its mutant versions were induced from the late L1 to late L3 stage (TS, Supplementary Fig. 3a). Micrococcal nuclease (+MN) was used to rule out the role of bacterial DNA in mediating the AbdA–Grh interaction in GST-Pulldown assay. Coomassie Blue gel depicts the loading of the GST-tagged protein samples. Bar = 20 μm. The graph shows mean ± SD. Significance is from a 2-tailed Student's unpaired *t*-test.

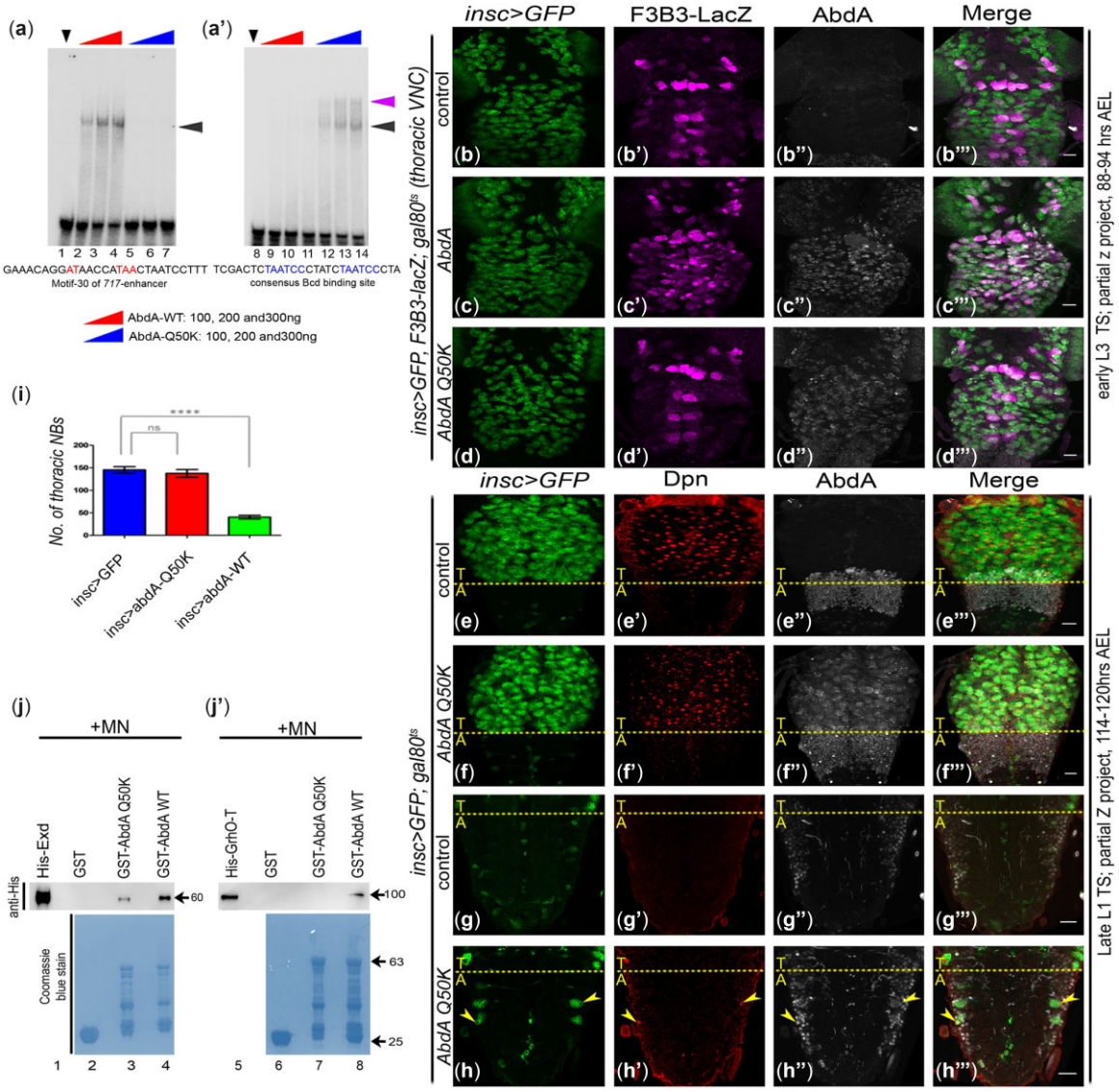

Fig. 5. Q50 residue in the AbdA-HD is crucial for its DNA-binding and apoptotic potential. a) EMSA showing that AbdA binds to motif 30 of the *717-enhancer* (lanes 2–4) while AbdA^{Q50K} fails to bind on this motif (lanes 5–7). a′) Conversely, AbdA^{Q50K} binds to the bicoid-binding site (lanes 12–14), while AbdA fails to do so (lanes 9–11). b-d) Compared to control (*insc>GFP*) (b′), ectopic expression of AbdA (*insc>AbdA*) induces apoptotic *F3B3-lacZ* (c′), while AbdA^{Q50K} (*insc>AbdA*^{Q50K}) fails to do so (d′) in thoracic NBs. e-h) Compared to controls (e–e‴; *insc>GFP*: 145 ± 7.1 NBs, $n = 12$ VNCs, $N = 3$), ectopic expression of AbdA^{Q50K} does not result in thoracic NB apoptosis (f–f‴; *insc> AbdA*^{Q50K}: 137.7 ± 8.5 NBs, $n = 12$ VNCs, $N = 3$) and instead blocks abdominal NB apoptosis in late L3 VNCs (g vs h). (i) Graph comparing the number of thoracic NBs in control vs. AbdA and AbdA^{Q50K} ectopic expression. (j–j′) Western blot shows that the Q50K mutation in AbdA-HD significantly decreases its interaction with Exd (lanes 3–4) and completely abolishes its interaction with Grh (lanes 7–8). Micrococcal nuclease (MN) treatment rules out the role of bacterial DNA in mediating these interactions. Coomassie Blue gel depicts the loading of the GST-tagged protein samples. Yellow arrowheads indicate abdominal NBs. Yellow dotted line separates the thoracic (T) and abdominal segments (A) of the VNC. In (b)–(d), ectopic expression for AbdA and AbdA^{Q50K} was induced for 8 hr (from early L3 to mid-L3 stage, TS, Supplementary Fig. 3d) to assay lacZ expression in these cells. The ectopic expression of AbdA^{Q50K} in (e)–(h) was induced from the late L1 to late L3 stage (TS, Supplementary Fig. 3a). Bar = 20 μm. The graph shows mean ± SD. Significance is from a 2-tailed Student's unpaired *t*-test. The DNA sequence used for EMSA is shown at the bottom of the gel pictures.

we also overexpressed the GrhO′ isoform to check the role of exon12b in the Grh function. We observed that both GrhO and GrhO′ overexpression resulted in a similar loss of thoracic NBs (Fig. 6b′ vs. Fig. 6, c′ and e′ and bars 2 and 3 in Fig. 6f), while GrhO$^{R204/207A}$ did not show any reduction; instead, a modest increase in the number of NBs was observed (Fig. 6b′ vs. Fig. 6d′ and bar 4 in Fig. 6f). This effect was comparable to the *grh* knockdown (Fig. 3e, bar 2). However, unlike the *grh* knockdown, GrhO$^{R204/207A}$ overexpression failed to block the abdominal NB apoptosis, possibly because the endogenous GrhO protein may be sufficient to bring about abdominal NB apoptosis. In order to check if GrhO was indeed dominant over GrhO$^{R204/207A}$, both proteins were simultaneously overexpressed (TS, Supplementary Fig. 3c). In this case, we found that the number of thoracic NBs was similar to that observed in case of GrhO alone (Supplementary Fig. 8, a–d). This suggests that overexpression of the R204/207 version cannot compromise the function of wild-type Grh.

We tested the interaction of the AbdA and GrhO$^{R204/207A}$ in vitro and observed that GST-AbdA could efficiently pull down both GrhO and GrhO$^{R204/207A}$ (lanes 5 and 6, Fig. 6h). This implied that mutagenesis of R204/207 residues did not significantly affect Grh's ability to interact with AbdA.

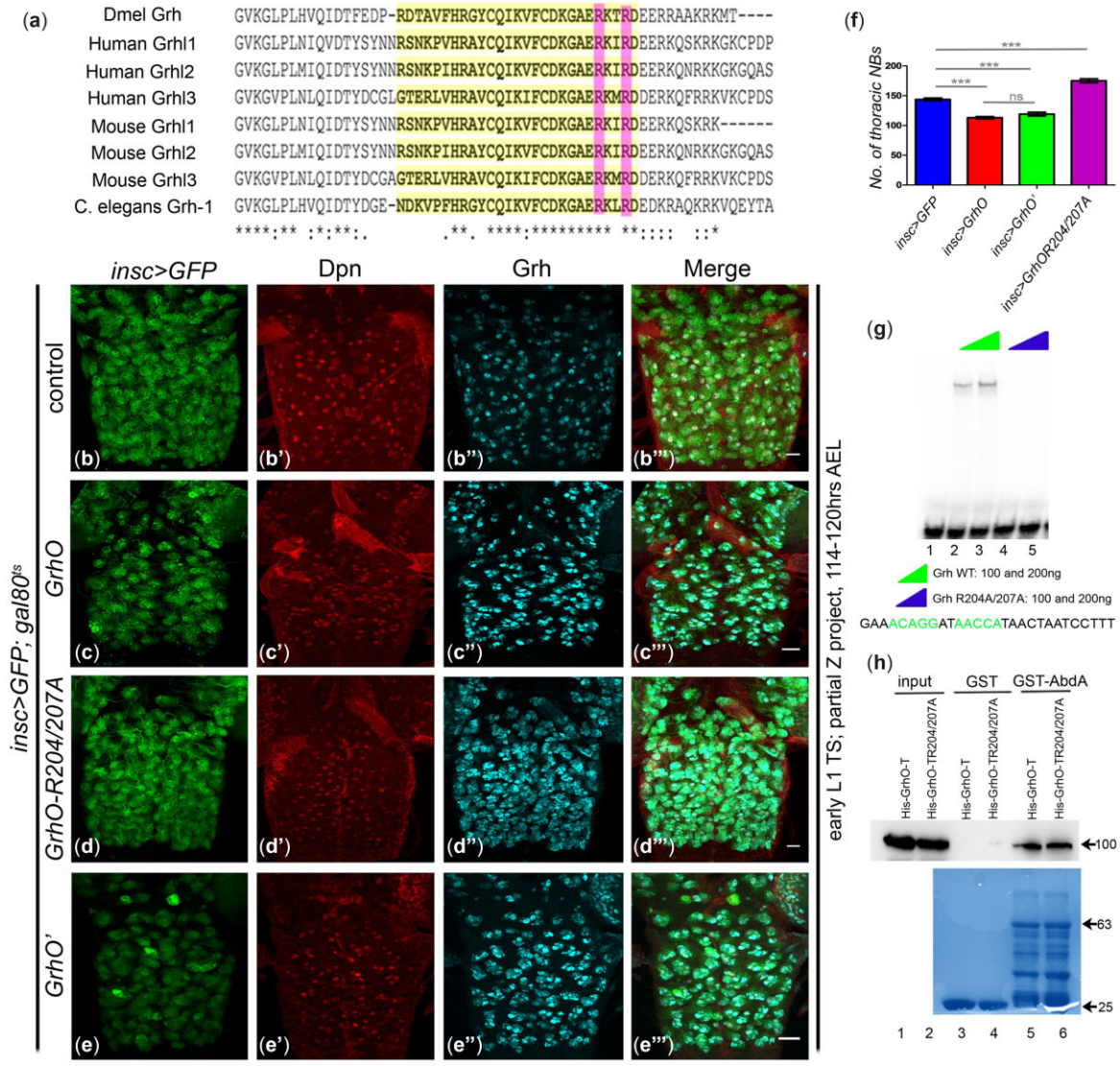

Fig. 6. Arginine 204/207 of the Grh-DBD are essential for its DNA binding and in vivo function. a) The alignment of a region from *Drosophila* Grh-DBD with its human, mouse, and *C. elegans* homologs. Residues 183–208 of the Grh-DBD (bold and highlighted) show high conservation (asterisks indicate conserved residues). Pink color highlights conserved arginine residues at positions 204 and 207. b–e) Compared to GFP expressing controls overexpression of GrhO and GrhO′ results in reduction in the number of thoracic NBs, while $GrhO^{R204/207A}$ results in an increase in the number of thoracic NBs, suggesting that mutation of R204/207A compromises Grh function in vivo. f) The graph comparing the number of thoracic NBs in control vs. overexpression of GrhO, GrhO′, and $GrhO^{R204/207A}$ (*insc*>GFP: 143.7 ± 6.29 NBs, $n = 12$ VNCs, $N = 3$; *insc*>*GrhO*: 113 ± 5.1 NBs, $n = 12$ VNCs, $N = 3$; *insc*>*GrhO′*: 119 ± 8.9 NBs, $n = 10$ VNCs, $N = 3$; *insc*>$GrhO^{R204/207A}$: 175 ± 8.9 NBs, $n = 12$ VNCs, $N = 3$). g) EMSA comparing the binding of 2 identical concentrations of Grh (lanes 2–3) and $Grh^{R204/207A}$ (lanes 4–5) on motif 30. R204/207A mutation compromise DNA-binding ability of Grh. h) Western blot shows that R204/207A mutation in Grh does not impact its interaction with AbdA (compare lanes 5 vs. 6). Coomassie Blue gel depicts the loading of the GST-tagged protein samples. The DNA sequence used for EMSA is shown at the bottom of the gel picture. The overexpression for GrhO, GrhO′, and $Grh^{R204/207}$ was induced from the early L1 to late L3 stage (TS, Supplementary Fig. 3c). Bar = 20 μm. The graph shows mean ± SD. Significance is from a 2-tailed Student's unpaired *t*-test.

These results show that the highly conserved arginine residues at positions 204/207 of Grh-DBD are critical for its DNA-binding ability in vitro and its function in vivo. Furthermore, the mutations of these residues did not disrupt its interaction with AbdA in vitro or confer dominant-negative properties to the Grh in vivo.

Hox-dependent apoptosis in Lab-SPG and Scr-SEG requires Grh

Hox-mediated NB apoptosis relies on Grh in Dfd, AbdA, and AbdB expressing regions of larval CNS (Cenci and Gould 2005; Khandelwal *et al.* 2017; Ghosh *et al.* 2019; Bakshi *et al.* 2020). To expand on the idea that Grh might play an essential role in NB apoptosis in other regions of CNS, we tested its expression and functional requirement in larval NB apoptosis in Lab-SPG and Scr-SEG.

Lab-SPG (shown in brown, Fig. 7a) has 12 NBs (6 NBs per hemisegment) in the L2 stage, of which 4 NBs (2 per hemisegment) (shown in purple, Fig. 7a) undergo Lab-dependent apoptosis in L2 to L3 transition (Kuert *et al.* 2012). To address the role of Grh in NB apoptosis in Lab-SPG, we costained larval CNS with Lab and Grh antibodies. In the L2 stage, we could consistently mark all the 12 NBs with both Lab and Grh (Fig. 7, b–b′) as reported earlier (Kuert *et al.* 2012). However, we could not detect consistent and significant Lab expression in NBs in the L3 stage (Fig. 7c′). We tested the expression of an enhancer trap line lab^{01241}-*lacZ* (BL-

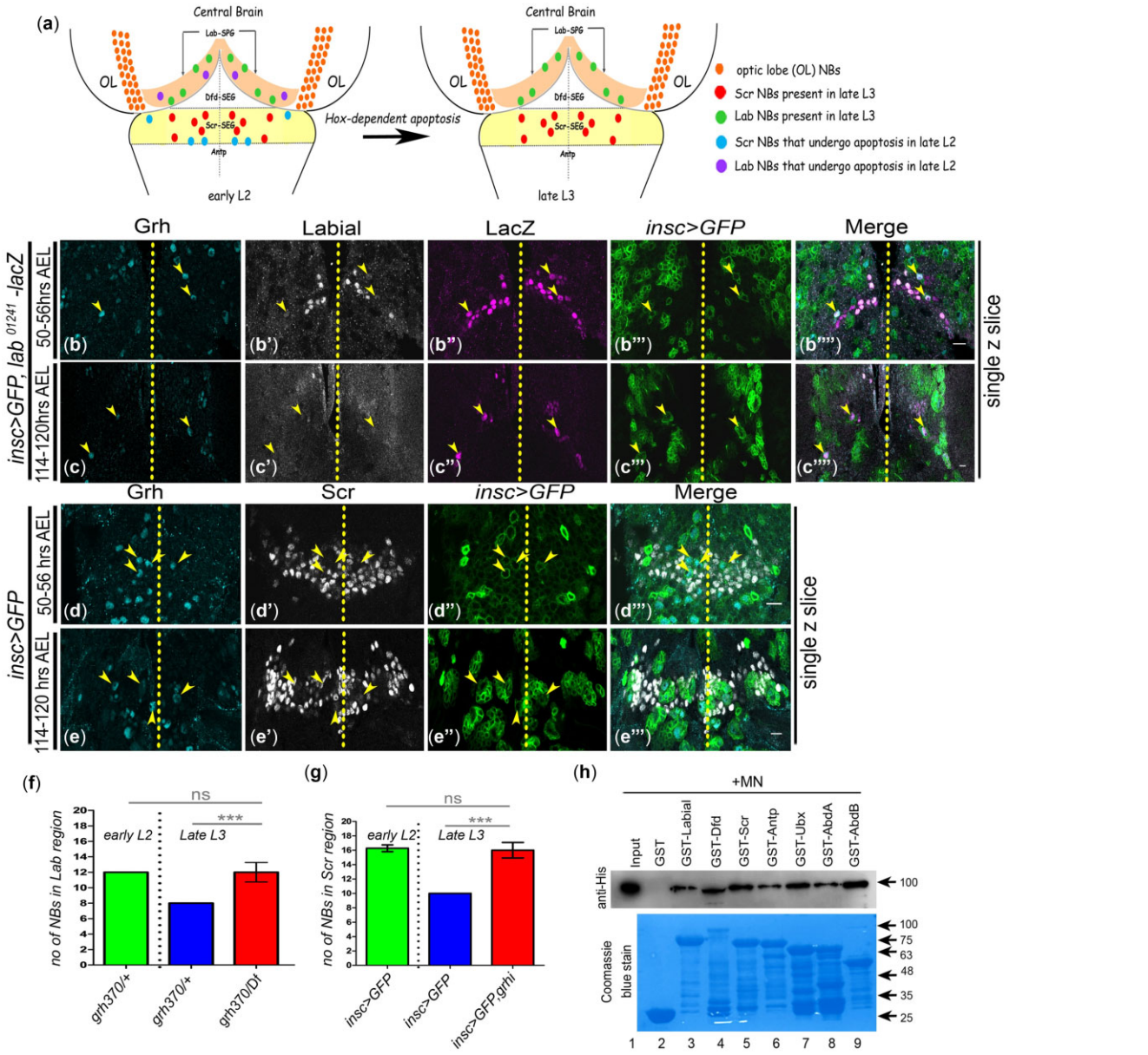

Fig. 7. Grh interacts with all Hox factors in vitro and is required for Hox-dependent NB apoptosis in Lab-SPG and Scr-SEG. a) Schematic of the larval CNS showing approximate positions of the NBs in Lab-SPG and Scr-SEG regions (shown in light brown and yellow, respectively) in the L2 and L3 stages of development. Lab-SPG region has 12 NBs (6 per hemisegment), of which 4 NBs (2 per hemisegment, shown in purple) undergo Lab-dependent apoptosis. This apoptosis leaves behind 8 NBs (4 per hemisegment shown in green) in the late L3 stages. Scr-SEG has 16 NBs (8 per hemisegment), of which 6 NBs (3 per hemisegment, shown in blue) undergo Scr-dependent apoptosis in L2 stages, leaving 10 NBs (5 per hemisegment, shown in red) in the late L3 stage. b-c) Expression of Grh and lab^{01241}-*lacZ* in NBs of Lab-SPG region in L2 (b–b‴) and L3 stage (c–c‴). The Lab-SPG region is marked by Lab staining, and lab^{01241}-*lacZ* is a consistent marker for NB and associated lineages in this region. d-e) Grh is expressed in the NBs of the Scr-SEG region of the CNS in L2 (d–d‴) and L3 stage (e–e‴). The Scr-SEG region is marked by Scr staining. f and g) The graphs showing that Lab and Scr-dependent NB apoptosis requires Grh. f) The graph shows the number of NBs observed in the Lab-SPG in L2 (grh^{370}/+; 12 ± 0 NBs, $n = 10$ CNS, $N = 3$) and L3 (grh^{370}/+; 8 ± 0 NBs, $n = 16$ CNS, $N = 3$) stages for heterozygous controls vs. heteroallelic *grh* mutant in L3 stage ($grh^{370/Df}$; 12 ± 1.3 NBs, $n = 11$ CNS, $N = 3$). g) The graph shows the number of NBs observed in Scr-SEG in L2 (*insc>GFP*; 16.2 ± 0.47 NBs, $n = 11$ CNS, $N = 3$) and L3 (*insc>GFP*; 10.3 ± 0.5 NBs, $n = 10$ CNS, $N = 3$) stage for control vs. *grh* knockdown (*insc>grh-RNAi*; 16 ± 1.1 NBs, $n = 16$ CNS, $N = 3$). The RNAi-mediated knockdown for *grh* was induced from the early L1 to late L3 stage (TS, Supplementary Fig. 3a). h) Western blot shows that all Hox factors can interact with Grh in vitro, the micrococcal nuclease (+MN) treatment rules out the role of bacterial DNA in this interaction. Coomassie Blue gel depicts the loading of the GST-tagged protein samples. A representative image of a single confocal slice of L2 and L3 stage VNC show only a subset of all the NBs. Supplementary Figs. 9 and 10 show all the NBs in the Lab-SPG and Scr-SEG regions. NBs are indicated by yellow arrowheads. The yellow dotted line represents the midline. Bar = 10 μm. The graph shows mean ± SD. Significance is from a 2-tailed Student's unpaired *t*-test.

11527) and found that it could successfully mark all the NBs and their progeny in the L2 ($n = 11$ CNS, $N = 3$, Fig. 7b″) and L3 stage ($n = 12$ CNS, $N = 3$, Fig. 7c″ and Supplementary Fig. 9b′). After that, we tested the genetic requirement of *grh* for NB apoptosis in Lab-SPG by using a heteroallelic combination of $grh^{370/Df}$. We observed that control (grh^{370}/+) CNS had 8 NBs in the late L3 stage (4 NBs per hemisegment, Supplementary Fig. 9, c–e, and bar 2 in Fig. 7f), while *grh* mutant CNS had 12 NBs (6 NBs per hemisegment, Supplementary Fig. 9, f–j, and bar 3 in Fig. 7f). This suggested a role of *grh* in Hox-dependent NB apoptosis in Lab-SPG.

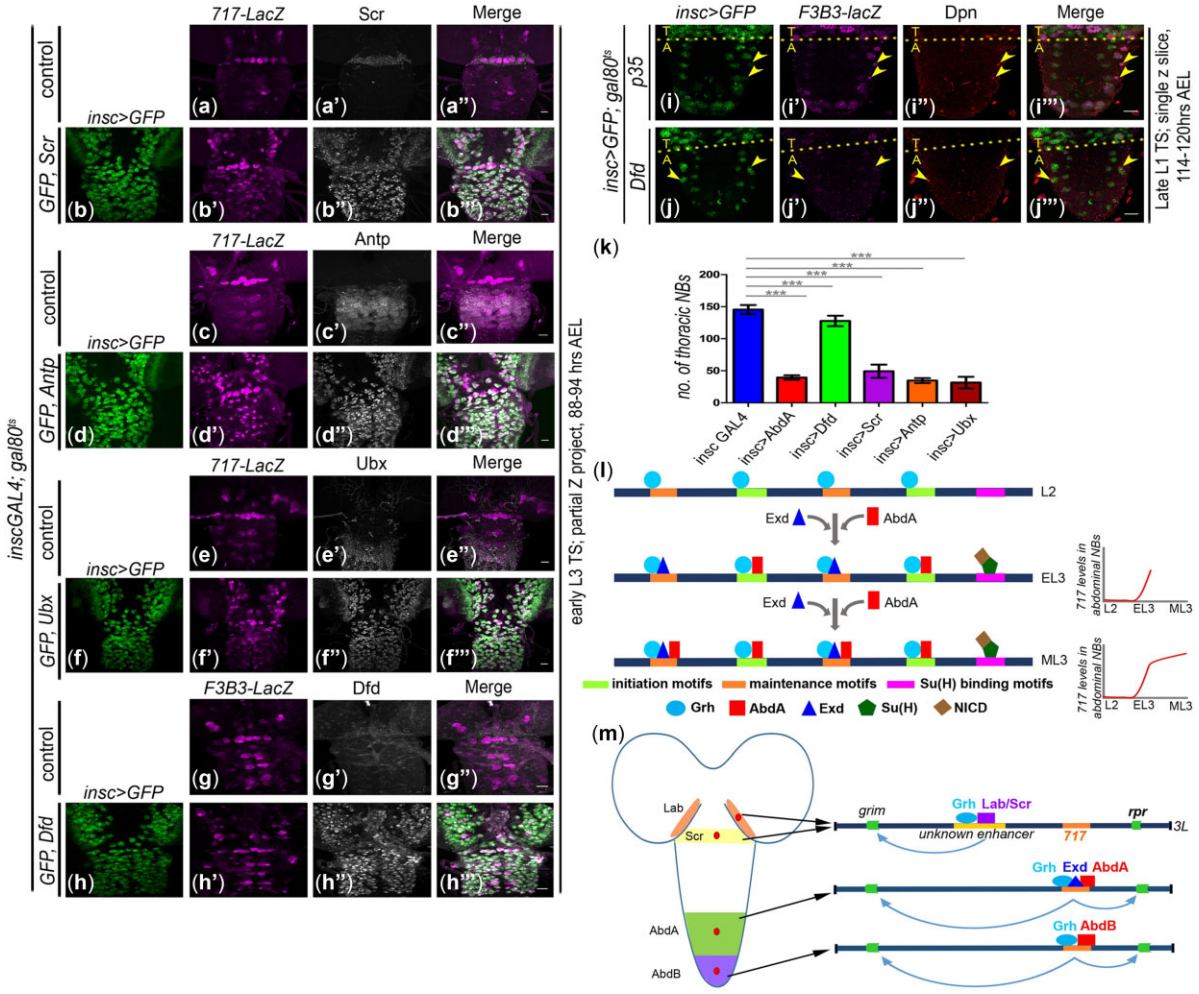

Fig. 8. Scr, Antp, Ubx, but not Dfd, induce thoracic NB apoptosis. a–f) Ectopic expression of Scr (b′), Antp (d′), and Ubx (f′) induces the *717-lacZ* expression in NBs of thoracic segments. The control VNCs with the basal expression of *717-lacZ* are also shown (a, c, and e, respectively). g–h) Ectopic expression of Dfd does not induce *F3B3-lacZ* in thoracic NBs (g vs. h′). The ectopic expression for Scr, Antp, Ubx, and Dfd was induced for 8 hr (from the early L3 to mid-L3 stage, TS, Supplementary Fig. 3d) in (a)–(h) to assay lacZ expression in NBs. i–j) Ectopic expression of Dfd (from late L1, TS, Supplementary Fig. 3a) in the abdominal NBs block their apoptosis in the late L3 stage (*insc>Dfd*; 30 ± 0 NBs, $n = 15$ VNCs, $N = 4$) (j″) and repress *F3B3-lacZ* (j′) in these cell; compared to this p35 expressing abdominal NBs in the control VNCs show the expression of *F3B3-lacZ* (i′). k) Graph compares the number of thoracic NB surviving in late L3 stage VNCs for control (*inscGAL4/+*; 145.5 ± 7.1 NBs, $n = 12$ VNCs, $N = 3$) and test which ectopically express different Hox factors from late L2 stage (TS, Supplementary Fig. 3b) (*insc>AbdA*; 39.45 ± 3.5 NBs, $n = 12$ VNCs, $N = 3$; *insc>Dfd*, 127.8 ± 8.2 NBs, $n = 13$ VNCs, $N = 3$; *insc>Scr*, 49.2 ± 10.3 NBs, $n = 12$ CNS, $N = 3$; *insc>Antp*, 34.8 ± 3.8 NBs, $n = 12$ VNCs, $N = 3$; *insc>Ubx*, 31.4 ± 9.1 NBs, $n = 8$ VNCs, $N = 3$). Ectopic expression of all the Hox factors except Dfd resulted in thoracic NB apoptosis. In (i) and (j), the ectopic expression for Dfd was *induced* from the late L1 to late L3 stage (TS, Supplementary Fig. 3a) to recover maximum number of NBs. a–h) The thoracic region of VNC is shown. i–j) The abdominal region of VNC is shown. Yellow arrowheads indicate NBs. The yellow dotted line separates the thoracic (T) and abdominal segments (A) of the VNC. Bar = 20μm. The graph shows mean ± SD. Significance is from a 2-tailed Student's unpaired *t*-test. l) A model of the apoptotic enhancer initiation and maintenance in the abdominal NBs is shown. Grh is bound to both initiation and maintenance motifs of the *717-enhancer*. In the early L3 stages, when a pulse of AbdA and Exd trigger apoptosis, AbdA occupies the initiation motifs and fires the *717-enhancer*. Following this, AbdA-Exd, and Grh maintain the enhancer activity through the maintenance motifs till NB undergoes apoptosis. The maintenance is also facilitated by Notch signaling through its effectors NICD and Su(H). m) Model showing that Hox-dependent NB apoptosis in different regions of developing CNS relies on Grh. The Hox factors AbdA and AbdB collaborate with Grh to activate the apoptotic genes *grim* and *rpr* in the abdominal and terminal NBs regions through the *717-enhancer*. In the anterior regions of the CNS, Grh and the Hox (Lab or Scr) promotes apoptosis of NBs primarily through activation of the apoptotic gene *grim* by using a different (yet to be identified) enhancer.

The Scr expressing region of SEG (Scr-SEG, shown in yellow, Fig. 7a) contains 16 NBs (8 NBs per hemisegment) in the L2 stage. Out of these, 6 NBs (3 per hemisegment, shown in blue color, Fig. 7a) undergo Scr-dependent apoptosis in the early L3 stage (Kuert *et al.* 2014). These NBs are easily identifiable based on their location within the Scr-SEG in the L2 stage (Fig. 7d). In the L3 stage, the NBs and the associated lineages showed Scr staining (Fig. 7e). We also observed that all the NBs in Scr-SEG (16 in the L2 stage and 10 surviving NBs in the L3 stage) expressed Grh (yellow arrowheads in Fig. 7, d and e).

Next, we tested the genetic requirement of Grh in NB apoptosis in Scr-SEG by RNAi-mediated *grh* knockdown (from the late L1 to late L3 stage, TS, Supplementary Fig. 3a). We recovered approximately 16 NBs in *grh* knockdown (Supplementary Fig. 10, d–g, and bar 3 in Fig. 7g) compared to controls (*insc>GFP*) which only had 10 NBs (Supplementary Fig. 10, a–c, and bar 2 in Fig. 7g), suggesting a role of *grh* in Scr-dependent apoptosis.

These results established a genetic requirement of Grh in all the regions of the CNS which exhibit Hox-dependent postembryonic NB apoptosis. Further, using deficiencies in chromosome

3 L (shown in Supplementary Fig. 11a), we find that *grim* is the primary gene responsible for the death of NBs in the Lab-SPG (Supplementary Data 7, Supplementary Fig. 11g, and bar 6 in Supplementary Fig. 11h) and Scr-SEG regions (Supplementary data 7, Supplementary Fig. 12e, and bar 5 in Supplementary Fig. 12f). Moreover, the enhancers responsible for activating *grim* in these regions are different from the *717-enhancer* and lie outside NBRR (Supplementary data 7 and Supplementary Figs. 11 and 12).

Since Grh is required in more than one region for Hox-dependent NB apoptosis (Khandelwal *et al.* 2017; Bakshi *et al.* 2020), we checked if it can interact with other Hox factors (Lab, Scr, Dfd, Antp, Ubx). We observed that while GST alone did not interact with His-tagged Grh (lane 2, Fig. 7h), all the GST-tagged Hox factors (Lab, Dfd, Scr, Antp, Ubx, AbdA, and AbdB) were capable of pulling down His-Grh (lanes 3–9, Fig. 7h).

These results show that Hox-dependent larval NB apoptosis in Lab-SPG and Scr-SEG critically relies on HLH TF Grh, and all 7 Hox proteins tested can physically interact with Grh.

Scr, Antp, and Ubx induce, while Dfd represses, thoracic NB apoptosis

Since Grh interacts with all the Hox proteins in vitro (Fig. 7h), we compared the relative apoptotic potential of different Hox factors and their capacity to induce *F3B3-lacZ* or *717-lacZ* in thoracic NBs prior to their death. We observed that ectopic expression of Scr (Fig. 8a vs. Fig. 8b′), Antp (Fig. 8c vs. Fig. 8d′), and Ubx (Fig. 8e vs. Fig. 8f′) induced *717-lacZ* in the NBs of the thorax and central brain in mid-L3 stage (TS, Supplementary Fig. 3d). Congruent with this, we observed a dramatic reduction in the number of surviving thoracic NBs and associated lineages (marked by *inscGAL4>GFP*) in these cases at L3 stage (TS, Supplementary Fig. 3b), compared to the control VNCs, which expressed only GFP (Fig. 8k and Supplementary Fig. 13, b–d).

In contrast to the results mentioned above, we observed that ectopic expression of Dfd neither induced *F3B3-lacZ* (Fig. 8g vs. Fig. 8h′) nor caused the apoptosis of thoracic NBs (Supplementary Fig. 13a and bar 3 in Fig. 8k). However, a block of NB apoptosis in the abdominal region was observed (Fig. 8j″). The surviving abdominal NBs did not express *F3B3-lacZ* (Fig. 8j′), while their counterparts in p35 expressing controls (p35 expression block apoptosis) showed lacZ expression (Fig. 8i′).

These results suggest that most Hox factors except Dfd can induce the *717-enhancer* that precedes thoracic NB apoptosis.

Discussion

In this study, we have investigated the role of Grh in Hox-mediated NB apoptosis that occurs in Lab, Scr, and AbdA expressing regions of larval VNC and show that Grh can function as a Hox cofactor. Mechanistically, we find that AbdA and Grh interact through their highly conserved DNA-binding domains and use a single 717-bp enhancer to activate abdominal NB apoptosis.

Different motifs mediate the initiation and maintenance of the *717-enhancer*

The *717-enhancer* relies on 2 separable sets of motifs for initiation and maintenance. Initiation motifs seem to be the first responders that activate the enhancer in response to increasing levels of AbdA (in the presence of Grh). This is followed by AbdA, Exd, Grh, and Notch taking over to sustain the activity of the enhancer through its maintenance motifs (Fig. 8l). A single enhancer for the initiation and maintenance of apoptotic gene expression is congruent with the fact that these genes are essential; however, their utility in the NBs is temporally limited to its death. Whether a single enhancer regulating apoptotic gene expression is a common feature of developmental apoptosis in *Drosophila* or vertebrates needs to be examined in detail.

Interestingly, both abdominal (A3–A7) and terminal (A8–A10) NBs in larval CNS use the same enhancer and overlapping molecular players (Hox-Grh-Notch) but employ different molecular strategies to activate apoptotic genes (Bakshi *et al.* 2020). In contrast to abdominal NBs, which use AbdA as a death trigger, the terminal NBs use elevated levels of Grh expression and Notch activity as the trigger (while keeping the expression of the resident Hox gene AbdB near-constant). Therefore, we expect that, like Hox-binding sites responsible for the initiation of the *717-enhancer* in the abdominal region, high-affinity Grh-binding sites may also exist on the enhancer, which may be used to trigger the enhancer in the terminal NBs. This idea fits our current observation that Grh is important for enhancer initiation in the abdominal region (Fig. 1). Conversely, there exists a possibility that initiation motifs bound by AbdA during abdominal NBs apoptosis may be bound by AbdB and used for enhancer initiation in the terminal NBs. Collectively, our data suggest that activation of RHG genes through the *717-enhancer* in abdominal and terminal NBs corroborates with the billboard model of enhancer function. In this model, a combination of TFs that bind to an enhancer is more important for the enhancer activity, rather than their exact arrangement and cooperativity (Kulkarni and Arnosti 2003; Rastegar *et al.* 2008; Junion *et al.* 2012; Smith *et al.* 2013).

Grh as an alternative cofactor for Hox function in vivo

The HLH protein and HD-containing TFs (Meis/Prep and Pitx family) are known to interact and synergize the transcriptional response (Knoepfler *et al.* 1999; Poulin *et al.* 2000), but the details of this interaction were unknown. We show that all the Hox factors (HD-TFs) can physically interact with Grh (bHLH-TF). More specifically, we find that AbdA and Grh collaborate through their highly conserved DNA-binding domains to execute abdominal NB apoptosis, and the specificity of the AbdA-HD is crucial for this interaction. We also show that Grh is required in all the regions of the CNS which exhibit Hox-dependent postembryonic NB apoptosis, supporting its role as a Hox cofactor.

The idea of Grh functioning as a potential Hox cofactor (Khandelwal *et al.* 2017) is also supported by a recent BioID study wherein Grh was found to interact with Ubx to promote the apoptosis of embryonic NBs in A1 and A2 segments (Carnesecchi *et al.* 2020). Similarly, in embryonic CNS, it is observed that many NBs express Grh but do not undergo apoptosis (Almeida and Bray 2005). This is possible considering that tissue and stage-specific function of Grh may depend on the recruitment of spatial factors (such as Hox) and/or temporal cues (such as the Notch signal). The idea gains support from the recent studies establishing Grh as a pioneer TF. These studies show that even though Grh remains bound to its targets across multiple stages, the (Grh-dependent) transcriptional profile changes (Nevil *et al.* 2017; Jacobs *et al.* 2018; Nevil *et al.* 2020).

Our prior work with larval NB apoptosis had shown that factors like Grh (Khandelwal *et al.* 2017; Bakshi *et al.* 2020) and Dsx (Ghosh *et al.* 2019) are capable of serving as alternative Hox

cofactors, especially in the terminal NBs where Exd is not essential (Ghosh *et al.* 2019; Bakshi *et al.* 2020). Revealing the latent specificity (as done by Exd for Hox factors) requires two TFs to interact cooperatively on the DNA (Slattery *et al.* 2011). Therefore, such a role for Dsx (which exhibits cooperative binding with AbdB) is possible but will be restricted to cells with a sex-specific fate. In the case of Grh, we find that AbdA–Grh interaction (on the *717-enhancer*) is not cooperative even in the presence of Exd (Khandelwal *et al.* 2017). However, such interaction (with or without Exd) may be possible on a different target gene in a different tissue. Considering its broad expression (Uv *et al.* 1997), we propose that Grh may function as a generic Hox cofactor across multiple tissues, but whether such collaborations happen in tissues other than the CNS needs to be examined.

Data availability

All relevant data are within the manuscript and its Supporting Information files.

Supplemental material is available at *GENETICS* online.

Acknowledgments

We thank Kristine White, S. Bray, R. Mann, J. Knoblich, K. Vijay Raghavan, S. Small, Sen-Lin Lai, C.Q. Doe, G. Hasan, L. S. Shashidhara, R. Mishra, T. Kundu, G. Ratnaparkhi, R. Rikhy, and D. Trivedi for various reagents and/or advice with experiments; BDSC, VDRC, NIG-Fly, and DGRC-Japan stock centers for fly lines; CDFD animal facility, Bioklone Biotech Pvt. Ltd., Chennai, and the Developmental Studies Hybridoma Bank at The University of Iowa for antibodies; and TFF at NCBS-CCAMP, Bangalore, for transgenic flies. We thank A. Ratnaparkhi and R. Kaur for the critical reading of the manuscript, A. Kunchur for her help with the anti-Exd antibody, A. Chinchole for his help with S2 cell culture, and C. S. Singh for his assistance in various phases of the project.

Funding

This study was funded by Department of Science and Technology, India (EMR/2016/003775, CRG/2021/003275); Department of Biotechnology, India (BT/PR26385/MED/122/110/2017, BT/PR27455/BRB/10/1647/2018, and BT/PR41306/MED/122/259/2020); Wellcome Trust DBT India Alliance, India (Ref: 500171/Z/09/Z) to RJ, CDFD core funds; and ICMR, India (award to RS) [ICMR Ref. No: 3/1/3/JRF-2012/HRD-63 (40260)].

Author contributions

RJ and RS conceptualized the study; RS did all the experiments; RS and RJ analyzed the data; and RJ and RS wrote the manuscript.

Conflicts of interest

None declared.

Literature cited

Affolter M, Percival-Smith A, Muller M, Leupin W, Gehring WJ. DNA binding properties of the purified Antennapedia homeodomain. Proc Natl Acad Sci U S A. 1990;87(11):4093–4097.

Akam M. Hox and HOM: homologous gene clusters in insects and vertebrates. Cell. 1989;57(3):347–349.

Almeida MS, Bray SJ. Regulation of postembryonic neuroblasts by Drosophila Grainyhead. Mech Dev. 2005;122(12):1282–1293.

Arya R, Sarkissian T, Tan Y, White K. Neural stem cell progeny regulate stem cell death in a Notch and Hox dependent manner. Cell Death Differ. 2015;22(8):1378–1387.

Baëza M, Viala S, Heim M, Dard A, Hudry B, Duffraisse M, Roguljа-Ortmann A, Brun C, Merabet S. Inhibitory activities of short linear motifs underlie Hox interactome specificity in vivo. eLife. 2015;4:e06034.

Bakshi A, Sipani R, Ghosh N, Joshi R. Sequential activation of Notch and Grainyhead gives apoptotic competence to Abdominal-B expressing larval neuroblasts in Drosophila Central nervous system. PLoS Genet. 2020;16(8):e1008976.

Bello BC, Hirth F, Gould AP. A pulse of the Drosophila Hox protein Abdominal-A schedules the end of neural proliferation via neuroblast apoptosis. Neuron. 2003;37(2):209–219.

Birkholz O, Rickert C, Berger C, Urbach R, Technau GM. Neuroblast pattern and identity in the Drosophila tail region and role of doublesex in the survival of sex-specific precursors. Development. 2013;140(8):1830–1842.

Bischof J, Duffraisse M, Furger E, Ajuria L, Giraud G, Vanderperre S, Paul R, Björklund M, Ahr D, Ahmed AW, *et al.* Generation of a versatile BiFC ORFeome library for analyzing protein-protein interactions in live Drosophila. eLife. 2018;7:e38853.

Carnesecchi J, Sigismondo G, Domsch K, Baader CEP, Rafiee M-R, Krijgsveld J, Lohmann I. Multi-level and lineage-specific interactomes of the Hox transcription factor Ubx contribute to its functional specificity. Nat Commun. 2020;11(1):1388.

Carroll SB. Homeotic genes and the evolution of arthropods and chordates. Nature. 1995;376(6540):479–485.

Cenci C, Gould AP. Drosophila Grainyhead specifies late programmes of neural proliferation by regulating the mitotic activity and Hox-dependent apoptosis of neuroblasts. Development. 2005;132(17):3835–3845.

Dasen JS, Liu JP, Jessell TM. Motor neuron columnar fate imposed by sequential phases of Hox-c activity. Nature. 2003;425(6961):926–933.

Dasen JS, Tice BC, Brenner-Morton S, Jessell TM. A Hox regulatory network establishes motor neuron pool identity and target-muscle connectivity. Cell. 2005;123(3):477–491.

Domsch K, Papagiannouli F, Lohmann I. The HOX-apoptosis regulatory interplay in development and disease. Curr Top Dev Biol. 2015;114:121–158.

Economides KD, Zeltser L, Capecchi MR. Hoxb13 mutations cause overgrowth of caudal spinal cord and tail vertebrae. Dev Biol. 2003;256(2):317–330.

Gebelein B, McKay DJ, Mann RS. Direct integration of Hox and segmentation gene inputs during Drosophila development. Nature. 2004;431(7009):653–659.

Ghosh N, Bakshi A, Khandelwal R, Rajan SG, Joshi R. The Hox gene Abdominal-B uses Doublesex(F) as a cofactor to promote neuroblast apoptosis in the Drosophila central nervous system. Development. 2019;146:dev175158.

Hart CP, Awgulewitsch A, Fainsod A, McGinnis W, Ruddle FH. Homeo box gene complex on mouse chromosome 11: molecular cloning, expression in embryogenesis, and homology to a human homeo box locus. Cell. 1985;43(1):9–18.

Hudry B, Remacle S, Delfini M-C, Rezsohazy R, Graba Y, Merabet S. Hox proteins display a common and ancestral ability to diversify their interaction mode with the PBC class cofactors. PLoS Biol. 2012;10(6):e1001351.

Jacobs J, Atkins M, Davie K, Imrichova H, Romanelli L, Christiaens V, Hulselmans G, Potier D, Wouters J, Taskiran II, *et al.* The transcription factor Grainy head primes epithelial enhancers for spatiotemporal activation by displacing nucleosomes. Nat Genet. 2018;50(7):1011–1020.

Junion G, Spivakov M, Girardot C, Braun M, Gustafson EH, Birney E, Furlong EEM. A transcription factor collective defines cardiac cell fate and reflects lineage history. Cell. 2012;148(3):473–486.

Khandelwal R, Sipani R, Govinda Rajan S, Kumar R, Joshi R. Combinatorial action of Grainyhead, Extradenticle and Notch in regulating Hox mediated apoptosis in Drosophila larval CNS. PLoS Genet. 2017;13(10):e1007043.

Knoepfler PS, Bergstrom DA, Uetsuki T, Dac-Korytko I, Sun YH, Wright WE, Tapscott SJ, Kamps MP. A conserved motif N-terminal to the DNA-binding domains of myogenic bHLH transcription factors mediates cooperative DNA binding with pbx-Meis1/Prep1. Nucleic Acids Res. 1999;27(18):3752–3761.

Kocak H, Ackermann S, Hero B, Kahlert Y, Oberthuer A, Juraeva D, Roels F, Theissen J, Westermann F, Deubzer H, *et al.* Hox-C9 activates the intrinsic pathway of apoptosis and is associated with spontaneous regression in neuroblastoma. Cell Death Dis. 2013; 4:e586.

Kuert PA, Bello BC, Reichert H. The labial gene is required to terminate proliferation of identified neuroblasts in postembryonic development of the Drosophila brain. Biol Open. 2012;1(10): 1006–1015.

Kuert PA, Hartenstein V, Bello BC, Lovick JK, Reichert H. Neuroblast lineage identification and lineage-specific Hox gene action during postembryonic development of the subesophageal ganglion in the Drosophila central brain. Dev Biol. 2014; 390(2):102–115.

Kulkarni MM, Arnosti DN. Information display by transcriptional enhancers. Development. 2003;130(26):6569–6575.

LaCount DJ, Hanson SF, Schneider CL, Friesen PD. Caspase inhibitor P35 and inhibitor of apoptosis Op-IAP block in vivo proteolytic activation of an effector caspase at different steps. J Biol Chem. 2000;275(21):15657–15664.

Lebrecht D, Foehr M, Smith E, Lopes FJP, Vanario-Alonso CE, Reinitz J, Burz DS, Hanes SD. Bicoid cooperative DNA binding is critical for embryonic patterning in Drosophila. Proc Natl Acad Sci U S A. 2005;102(37):13176–13181.

Lelli KM, Noro B, Mann RS. Variable motif utilization in homeotic selector (Hox)-cofactor complex formation controls specificity. Proc Natl Acad Sci U S A. 2011;108(52):21122–21127.

Mann RS, Affolter M. Hox proteins meet more partners. Curr Opin Genet Dev. 1998;8(4):423–429.

Mann RS, Chan SK. Extra specificity from extradenticle: the partnership between HOX and PBX/EXD homeodomain proteins. Trends Genet. 1996;12(7):258–262.

Mann RS, Lelli KM, Joshi R. Hox specificity unique roles for cofactors and collaborators. Curr Top Dev Biol. 2009;88:63–101.

Maurange C, Cheng L, Gould AP. Temporal transcription factors and their targets schedule the end of neural proliferation in Drosophila. Cell. 2008;133(5):891–902.

Merabet S, Litim-Mecheri I, Karlsson D, Dixit R, Saadaoui M, Monier B, Brun C, Thor S, Vijayraghavan K, Perrin L, *et al.* Insights into Hox protein function from a large scale combinatorial analysis of protein domains. PLoS Genet. 2011;7(10):e1002302.

Merabet S, Mann RS. To be specific or not: the critical relationship between Hox and TALE proteins. Trends Genet. 2016;32(6):334–347.

Merabet S, Saadaoui M, Sambrani N, Hudry B, Pradel J, Affolter M, Graba Y. A unique Extradenticle recruitment mode in the Drosophila Hox protein Ultrabithorax. Proc Natl Acad Sci U S A. 2007;104(43):16946–16951.

Miguel-Aliaga I, Thor S. Segment-specific prevention of pioneer neuron apoptosis by cell-autonomous, postmitotic Hox gene activity. Development. 2004;131(24):6093–6105.

Ming Q, Roske Y, Schuetz A, Walentin K, Ibraimi I, Schmidt-Ott KM, Heinemann U. Structural basis of gene regulation by the Grainyhead/CP2 transcription factor family. Nucleic Acids Res. 2018;46(4):2082–2095.

Moens CB, Selleri L. Hox cofactors in vertebrate development. Dev Biol. 2006;291(2):193–206.

Neumüller RA, Richter C, Fischer A, Novatchkova M, Neumüller KG, Knoblich JA. Genome-wide analysis of self-renewal in Drosophila neural stem cells by transgenic RNAi. Cell Stem Cell. 2011;8(5): 580–593.

Nevil M, Bondra ER, Schulz KN, Kaplan T, Harrison MM. Stable binding of the conserved transcription factor grainy head to its target genes throughout Drosophila melanogaster development. Genetics. 2017;205(2):605–620.

Nevil M, Gibson TJ, Bartolutti C, Iyengar A, Harrison MM. Establishment of chromatin accessibility by the conserved transcription factor Grainy head is developmentally regulated. Development. 2020;147:dev185009.

Nguyen TN, Goodrich JA. Protein-protein interaction assays: eliminating false positive interactions. Nat Methods. 2006;3(2):135–139.

Noyes MB, Christensen RG, Wakabayashi A, Stormo GD, Brodsky MH, Wolfe SA. Analysis of homeodomain specificities allows the family-wide prediction of preferred recognition sites. Cell. 2008; 133(7):1277–1289.

Poulin G, Lebel M, Chamberland M, Paradis FW, Drouin J. Specific protein-protein interaction between basic helix-loop-helix transcription factors and homeoproteins of the Pitx family. Mol Cell Biol. 2000;20(13):4826–4837.

Prokop A, Bray S, Harrison E, Technau GM. Homeotic regulation of segment-specific differences in neuroblast numbers and proliferation in the Drosophila central nervous system. Mech Dev. 1998; 74(1–2):99–110.

Rastegar S, Hess I, Dickmeis T, Nicod JC, Ertzer R, Hadzhiev Y, Thies W-G, Scherer G, Strähle U. The words of the regulatory code are arranged in a variable manner in highly conserved enhancers. Dev Biol. 2008;318(2):366–377.

Regulski M, Harding K, Kostriken R, Karch F, Levine M, McGinnis W. Homeo box genes of the Antennapedia and bithorax complexes of Drosophila. Cell. 1985;43(1):71–80.

Saadaoui M, Merabet S, Litim-Mecheri I, Arbeille E, Sambrani N, Damen W, Brena C, Pradel J, Graba Y. Selection of distinct Hox-Extradenticle interaction modes fine-tunes Hox protein activity. Proc Natl Acad Sci U S A. 2011;108(6):2276–2281.

Saurin AJ, Delfini MC, Maurel-Zaffran C, Graba Y. The generic facet of Hox protein function. Trends Genet. 2018;34(12):941–953.

Slattery M, Riley T, Liu P, Abe N, Gomez-Alcala P, Dror I, Zhou T, Rohs R, Honig B, Bussemaker HJ, *et al.* Cofactor binding evokes latent differences in DNA binding specificity between Hox proteins. Cell. 2011;147(6):1270–1282.

Smith RP, Taher L, Patwardhan RP, Kim MJ, Inoue F, Shendure J, Ovcharenko I, Ahituv N. Massively parallel decoding of mammalian regulatory sequences supports a flexible organizational model. Nat Genet. 2013;45(9):1021–1028.

Tabuse M, Ohta S, Ohashi Y, Fukaya R, Misawa A, Yoshida K, Kawase T, Saya H, Thirant C, Chneiweiss H, *et al.* Functional analysis of HOXD9 in human gliomas and glioma cancer stem cells. Mol Cancer. 2011;10:60.

Tan Y, Yamada-Mabuchi M, Arya R, St Pierre S, Tang W, Tosa M, Brachmann C, White K. Coordinated expression of cell death genes regulates neuroblast apoptosis. Development. 2011; 138(11):2197–2206.

Treisman J, Gonczy P, Vashishtha M, Harris E, Desplan C. A single amino acid can determine the DNA binding specificity of homeodomain proteins. Cell. 1989;59(3):553–562.

Truman JW, Bate M. Spatial and temporal patterns of neurogenesis in the central nervous system of Drosophila melanogaster. Dev Biol. 1988;125(1):145–157.

Uv AE, Harrison EJ, Bray SJ. Tissue-specific splicing and functions of the Drosophila transcription factor Grainyhead. Mol Cell Biol. 1997;17(11):6727–6735.

Communicating editor: V. Meller